



**NUMERICAL INVESTIGATION ON THE
COOLING OF HAWT NACELLA**

**2022
MASTER THESIS
MECHANICAL ENGINEERING**

Abdulkhaliq Salman Mwaea ALKAABI

**Thesis Advisor
Asst. Prof. Dr. Mehmet BAKIRCI**

NUMERICAL INVESTIGATION ON THE COOLING OF HAWT NACELLA

Abdulkhaliq Salman Mwaea ALKAABI

**T.C.
Karabuk University
Institute of Graduate Programs
Department of Mechanical Engineering
Prepared as
Master Thesis**

**Thesis Advisor
Asst. Prof. Dr. Mehmet BAKIRCI**

**KARABÜK
November 2022**

I certify that in my opinion the thesis submitted by Abdulkhaliq Salman Mwhea ALKAABI titled "NUMERCAL INIVESTIGATION ON THE COOLING OF HAWT NACELLA " is fully adequate in scope and quality as a thesis for the degree of Master of Science.

Asst. Prof. Dr. Mehmet BAKIRCI
Thesis Advisor, Department of Mechanical Engineering

This thesis is accepted by the examining committee with a unanimous vote in the Department of Mechanical Engineering as a Master of Science thesis. 10/10/ 2022

Examining Committee Members (Institutions) Signature

Chairman : Prof. Dr. Emrah Deniz (KBÜ)

Member : Prof. Dr. Ahmet KABUL (ISUBÜ)

Member : Asist. Prof. Dr. Mehmet BAKIRCI (KBÜ)

The degree of Master of Science by the thesis submitted is approved by the Administrative Board of the Institute of Graduate Programs, Karabuk University.

Prof. Dr. Hasan SOLMAZ
Director of the Institute of Graduate Programs

“I declare that all the information within this thesis has been gathered and presented in accordance with academic regulations and ethical principles and I have according to the requirements of these regulations and principles cited all those which do not originate in this work as well.”

Abdulkhaliq Salman Mwhea ALKAABI

ABSTRACT

M. Sc. Thesis

NUMERICAL INVESTIGATION ON THE COOLING OF HAWT NACELLA

Abdulkhaliq Salman Mwhea ALKAABI

Karabuk University

Institute of Graduate Programs

The Department of Mechanical Engineering

Thesis Advisor:

Asst. Prof. Dr. Mehmet BAKIRCI

October 2022, 63 page

Wind turbines have to keep running even when the weather is bad and the temperatures fluctuate throughout the day and the year. Most noticeably, the nacelle's electrical and electronic components could be subjected to extreme temperature changes, which could cause strains in the design that are inconsistent with the intended operation of the components. A manageable temperature inside the nacelle can be maintained by rejecting to the atmosphere the heat produced by the electrical and mechanical components as a result of various power dissipations (due to the Joule effect, friction losses released (generator, gearbox)). This is accomplished by regulating the heat exchange between the nacelle's internal air and the air outside. In this study, a liquid cooling system and forced air Cooling system were used to cool the mechanical and electrical equipment. The effectiveness of cooling was evaluated by a comparison utilizing the simulation program. The Reynolds-averaged Navier-Stokes equations describe the flow of air into and out of the nacelle, as well as the flow of liquid in and out. Heat transmission has been factored in using the energy

equation. The Result includes the temperature for the gearbox and generator by used a liquid and air forced cooling system. The results of the simulations showed that liquid cooling is superior to forced air cooling. Specifically, the significance of designing and implementing an effective cooling system for nacelle temperature control is given and explored.

Key Words : Wind turbine, Nacelle, air-forced cooling system, liquid cooling system, Computational Fluid Dynamics.

Science Code : 91411

ÖZET

Yüksek Lisans Tezi

HAWT NACELLA'NIN SOĞUTULMASI ÜZERINE SAYISAL ARAŞTIRMA

Abdulkhaliq Salman Mwaea ALKAABI

Karabük Üniversitesi

Lisansüstü Eğitim Enstitüsü

Makina Mühendisliği Anabilim Dalı

Tez Danışmanı:

Dr. Öğr. Üyesi Mehmet BAKIRCI

Ekim 2022, 63 sayfa

Rüzgar türbinleri, hava kötü olduğunda ve sıcaklıklar gün ve yıl boyunca dalgalandığında bile çalışmaya devam etmek zorundadır. En dikkat çekici olanı, naselin elektrikli-elektronik ve mekanik bileşenleri, çalışma performanslarını düşüren aşırı mekanik gerilimlere neden olabilecek yüksek sıcaklık değerlerine maruz kalabilirler. Rüzgar türbininde oluşacak güç kayıplarını engellemek amacıyla sıcaklık değerlerini istenilen düzeyde tutmak için, elektrik ve mekanik bileşenler tarafından üretilen ısının atmosfere atılarak, navel içinde yönetilebilir bir sıcaklık elde edilebilir. Bu, naselin iç havası ile dışarıdaki hava arasındaki ısı alışverişini düzenleyerek gerçekleştirilir. Bu çalışmada, mekanik ve elektrikli ekipmanların soğutulması için sıvı soğutma sistemi ve cebri hava soğutma sistemi kullanılmıştır. Soğutmanın etkinliği, hesaplamalı akışkanlar dinamiğini(HAD) kullanan simülasyon programı kullanılarak bir karşılaştırma yapılarak değerlendirildi. Reynolds ortalımalı Navier-Stokes denklemleri, havanın naselin içine ve dışına akışının yanı sıra sıvının içeri ve dışarı akışını tanımlar. Enerji denklemi kullanılarak ısı iletimi hesaba katılmıştır.

Sonuç olarak, kullanılan sıvı ve hava soğutma sistemi ile dişli kutusu ve jeneratör sıcaklığının istenilen seviyede tutulması sağlanabildiği görülmüştür. Simülasyonların sonuçları, sıvı soğutmanın hava soğutmaya göre daha üstün olduğunu göstermiştir. Bu çalışmada, nanel sıcaklık kontrolü için etkili bir soğutma sistemi tasarlanmasının ve uygulamanın önemi verilmiş ve araştırılmıştır.

Anahtar Kelimeler : Rüzgar Türbini, Nacelle, Cebri hava soğutma sistemi, sıvı soğutma sistemi, Hesaplama Akışkanlar Dinamiği.

Bilim Kodu : 91411

ACKNOWLEDGMENT

In the name of Allah, the Merciful

Praise be to Allah, Lord of the Worlds, for his bounty and generosity, providing me with the strength and determination to finish this work. I also want to express my sincere gratitude to my direct supervisor "Assist. Prof. Dr. Mehmet BAKIRCI " for the support he provided me through his continuous guidance, useful advice, patience, and support throughout the writing of this thesis.

I'm also grateful for my mother's prayers for me and my family, as well as my brothers and friends, who have helped me overcome all of the obstacles I've faced. I also dedicate this effort to future scholars in order for them to profit from and improve the content as much as feasible.

CONTENTS

	<u>Page</u>
APPROVAL.....	ii
ABSTRACT.....	iv
ÖZET.....	vi
ACKNOWLEDGMENT.....	viii
CONTENTS.....	ix
LIST OF FIGURES	xi
LIST OF TABLES	xiii
SYMBOLS AND ABBREVIATIONS	xiv
PART 1	1
INTRODUCTION	1
1.1. WIND TURBINE COMPENENT	3
1.2. LITERATURE REVIEW	4
PART 2	19
THEORETICAL AND NUMERICAL ANALYSIS	19
2.1. MODELLING AND SIMULATION.....	19
2.1.1. Computational Fluid Dynamics (CFD)	19
2.1.2. Ansys Fluent	20
2.2. PROBLEM DESCRIPTION	20
2.3. DESCRIPTION OF THE PHYSICAL MODEL	21
2.3.1. Air Forced Cooling System	21
2.3.2. Liquid Cooling System.....	22
2.4. ASSUMPTION AND MATRAEIL PROPERTIES.....	22
2.5. CFD SIMULATION	23
2.6. GOVERNING EQUATIONS	26
PART 3	30
RESULT AND DISCUSTION	30
3.1. INTRODUCTION.....	30

	<u>Page</u>
3.2. FORCED AIR-COOLING SYSTEM	31
3.2.1. Air Tempurture 20 °C	31
3.2.2. Air Tempurture 40 °C	37
3.3. LIQUID COOLING SYSTEM	42
3.3.1. Liquid Tempurture 20 °C	43
3.3.2. Liquid Tempurture 30 °C	49
3.3. COMPARISON BETWEEN THE RESULTS FOR AIR FORCED COOLING SYSTEM AND LIQUID COOLING SYTEM	55
 PART 4	 58
CONCLUSION	58
4.1. SUGGESTIONS FOR FUTURE STUDY	59
 REFERENCE.....	 60
 RESUME	 63

LIST OF FIGURES

	<u>Page</u>
Figure 1.1. Nacelle wind turbine.....	3
Figure 2.1. Air forced cooling system.....	21
Figure 2.2. Jet cooler for generator.....	22
Figure 2.3. View mesh for air cooling system.....	24
Figure 2.4. View mesh for liquid cooling system.....	25
Figure 3.1. Velocity contour for 3m/s.....	31
Figure 3.2. Velocity contour for 5m/s.....	32
Figure 3.3. Velocity contour for 7m/s.....	33
Figure 3.4. Variation of mass flow (Kg/s) rate and temperature (°C).....	34
Figure 3.5. Variation of mass flow (Kg/s) rate and heat transfer (KW).....	35
Figure 3.6. Temperature distribution for generator and gear box in 20°C for 3 m/s.....	35
Figure 3.7. Temperature distribution for generator and gear box in 20°C for 5 m/s.....	36
Figure 3.8. Temperature distribution for generator and gear box in 20°C for 5 m/s.....	36
Figure 3.9. Case I velocity contour for 3m/s.....	37
Figure 3.10. Velocity contour for 5m/s.....	38
Figure 3.11. Velocity contour for 7m/s.....	39
Figure 3.12. Variation of mass flow (Kg/s) rate and temperature (°C).....	40
Figure 3.13. Variation of mass flow (Kg/s) rate and heat transfer (KW).....	41
Figure 3.14. Temperature distribution for generator and gear box in 3m/s.....	41
Figure 3.15. Temperature distribution for generator and gear box in 5m/s.....	42
Figure 3.16. Temperature distribution for generator and gear box in 7m/s.....	42
Figure 3.17. Variation of mass flow (Kg/s) rate and temperature for the gearbox (°C).....	44
Figure 3.18. Variation of mass flow rate (Kg/s) and temperature for generator (°C).....	44
Figure 3.19. Variation of mass flow rate (Kg/s) for oil and heat transfer (kw).....	45
Figure 3.20. Variation of mass flow rate (Kg/s) for water and heat transfer (kw).....	45
Figure 3.21. Temperature distribution for generator in 20°C in 0.0005m/s.....	46
Figure 3.22. Temperature distribution for generator in 20°C in 0.001m/s.....	46

	<u>Page</u>
Figure 3.23. Temperature distribution for generator in 20°C in 0.0015m/s.....	47
Figure 3.24. Temperature distribution for gearbox in 20°C in 0.0005m/s.....	47
Figure 3.25. Temperature distribution for gearbox in 20°C in 0.001m/s.....	48
Figure 3.26. Temperature distribution for gearbox in 20°C in 0.0015m/s.....	48
Figure 3.27. Variation of mass flow (Kg/s) rate and temperature for gearbox (°C)..	50
Figure 3.28. Variation of mass flow rate (Kg/s) and temperature for generator (°C).	50
Figure 3.29. Variation of mass flow rate (Kg/s) for oil and heat transfer (kw).	51
Figure 3.30. Variation of mass flow rate (Kg/s) for water and heat transfer (kw)....	51
Figure 3.31. Temperature distribution for generator 30°C in 0.0005 m/s.....	52
Figure 3.32. Temperature distribution for generator 30°C in 0.001m/s.....	52
Figure 3.33. Temperature distribution for generator 30°C in 0.0015m/s.....	53
Figure 3.34. Temperature distribution for gearbox 30°C in 0.0005m/s.....	53
Figure 3.35. Temperature distribution for gearbox 30°C in 0.001m/s.....	54
Figure 3.36. Temperature distribution for gearbox 30°C in 0.0015.....	54
Figure 3.37. Comparison between the temperature of the generator cooled by the air forced system and the liquid cooling system.	55
Figure 3.38. Comparison between the temperature of the generator cooled by the air forced system and the liquid cooling system.	56
Figure 3.39. Comparison between the temperature of the gearbox cooled by the air forced system and the liquid cooling system.	57
Figure 3.40. Comparison between the temperature of the gearbox cooled by the air forced system and the liquid cooling system.	57

LIST OF TABLES

	<u>Page</u>
Table 1.1. Summary of the literature review.....	12
Table 2.1. Property for the material.	23
Table 2.2. Mish-applied option for geometry in air cooling system.....	24
Table 2.3. Mish-applied option for geometry in the liquid cooling system.....	25
Table 2.4. The impact of grid element size on the data obtained.....	26
Table 2.5. Gives the values of the empirical constants for (k - ϵ) modelling.	29
Table 3.1. Temperature data for case I.....	31
Table 3.2. Temperature data for case II.	32
Table 3.3. Temperature data for case III.	33
Table 3.4. Temperature data for case I.....	37
Table 3.5. Temperature data for case II.	38
Table 3.6. Temperature data for case III.	39
Table 3.7. Temperature data for liquid cooling system in 20 °C.....	43
Table 3.8. Temperature data for liquid cooling 30 °C.	49

SYMBOLS AND ABBREVIATIONS

SYMBOL

K	: Thermal conductivity
C_p	: Specific heat
m°	: Mass flow rate
A	: Section area
w	: Velocity in z-axis
v	: Velocity in Y-axis
u	: Velocity in x-axis
ρ	: Density
σ	: Absorptivity
α	: diffusion coefficient
μ	: Dynamic viscosity
T	: Temperature
T_{avg}	: Average temperature
h	: Heat transfer coefficient
$\sigma_k \sigma_\varepsilon$: Turbulent Prandtl numbers for k , ε
P	: Mean static pressure
p_r	: Prandtl number
ν_t	: Eddy or turbulent viscosity
ν_e	: Effective kinematics viscosity
ε	: Dissipation rate of turbulent kinetic energy
Q	: Thermal energy transferred
q	: Heat flux
x, y, z	: Cartesian coordinate
r, θ, z	: Cylindrical-coordinate

ABBREVIATIONS

CC : Cold climate

CFD : Computational Fluid Dynamics

DFIG : Doubly-fed induction generator

HAWT: Horizontal-Axis Wind Turbine

K- ε : Two-equations turbulence model

NSE : Navier stock equation

WTHE: Wind tower heat exchanger

PART 1

INTRODUCTION

Renewable energy increased from 20% to 28% of worldwide electricity supply between 2011 and 2021. Fossil energy fell from 68% to 62%, while nuclear energy fell from 12% to 10%. Hydropower's proportion fell from 16% to 15%, while solar and wind power climbed from 2% to 10%. Biomass and geothermal energy increased from 2% to 3% of total energy use. There are 3,146 gigatons of installed renewable energy capacity in 135 nations, with 156 countries having legislation governing the renewable energy industry [1]. Wind energy is one of the most rapidly expanding renewable energy industries. This evolution has produced a demand for increasingly accurate and efficient wind models during the previous few decades. For energy generation, wind turbines with capacities ranging from 1MW to 6MW are available. Wind turbine capacity, either directly or indirectly, relies on the cooling effect of the cooling systems supplied for wind turbine components. Wind turbine capacity can be enhanced if the components can perform properly without overheating for an extended length of time. Thus, boosting the effectiveness of a wind turbine's cooling system is critical in the development of wind turbine designs [2]. In addition, wind turbines in cold regions are subjected to icing conditions and low temperatures that exceed the design limits of typical wind turbines. Standard turbines working in such harsh settings are prone to production losses and higher loads, which increases the danger of early mechanical failure and financial losses. CC locations are areas where icing occurrences or periods with temperatures below the operational limitations of typical wind turbines occur, which can have an influence on project execution, economics, and safety [3]. Most wind turbine cooling systems use a forced flow of external air as a heat transfer fluid. This flow either directly cools the electrical and mechanical components or flows via an air/liquid heat exchanger, which is typically situated on the nacelle's top/back side. For turbines that operate in severe conditions, manufacturers commonly utilize liquid-cooled generators. These generators are more

compact than air-cooled generators and have improved electrical efficiency due to superior cooling and decreased drag/friction losses [4]. In this study, the focus is on cooling the gearbox and generator because of the waste heat generated by the gearbox and generator. The heat load in the gearbox mostly elevates the temperature of the oil. The heat is mostly created by the gearbox operation, which converts a portion of the kinetic energy into heat energy, causing the temperature to rise. As the temperature rises, the viscosity of the oil decreases and thins, destroying the lubricating oil coating, and increasing gear friction and calorific value, culminating in a vicious cycle. And if the temperature is too high, the tooth surface bonding causes damage to the gear and perhaps large losses. As a result, efficient heat exchange between the gearbox and cooling fluid is required to guarantee normal functioning. The heat load of the generator is caused by copper loss, which is caused by generator components around the winding copper wires; iron loss, which is caused by the rotation of the core hysteresis effect of eddy current, resulting in hysteresis loss and eddy current loss; and mechanical loss, which is caused by the energy used to overcome friction during generator operation. All of this energy loss will be converted into thermal energy and transferred to the wind turbine nacelle [5]. Wind turbine cooling technology is separated into two types: air cooling systems and liquid cooling systems. Furthermore, air cooling systems are classified as either natural ventilation cooling or forced air cooling. According to statistics, around 95% of wind turbines use forced air cooling or liquid cooling [6]. The purpose of this study is to determine the optimal cooling strategy for the generator and gearbox using an air-forced cooling system and liquid cooling systems. Computational fluid dynamic (CFD) software was used to derive temperature values. Detailed results, including the temperature for generator and gearbox in the nacelle under wind velocity (3, 5, 7) m/s for inlet air in forced air-cooling system and three velocities for liquid cooling system (0.0005, 0.001, 0.0015) m/s. The airflow is modeled using Reynolds averaged Navier-Stokes equations for cartesian coordinate and cylindrical coordinate in this technique. Heat transport effects are accounted for by using the energy equation. For the description of turbulent flow, the standard k-epsilon model was adopted.

1.1. WIND TURBINE COMPENENT

The main shaft is attached to the blades of a wind turbine. Premium, heat-treated steel is used in its construction. We hollowed it out to save on weight without compromising durability. A gearbox is linked to the primary shaft. The gearbox is often seen in wind turbine is used to enhance the rotational speed of a rotor in a low-speed generating system so that it can be used to generate electricity at a higher rate. A typical ratio of 90:1 would have the rotor turning at 20 rpm and the generator spinning at 1,500 rpm. The link between the gearbox and the generator allows for the transfer of power. Shafts can exchange rotational power using mechanical couplings. A high-speed shaft may be somewhat out of alignment due to the connection that is part of the design. It is necessary to employ flexible couplings on the high-speed (output) shaft of the gearbox in order to drive the generator and account for the misalignment between the two in wind turbines. These parts need to be cooled since they get hot from constant spinning and friction.

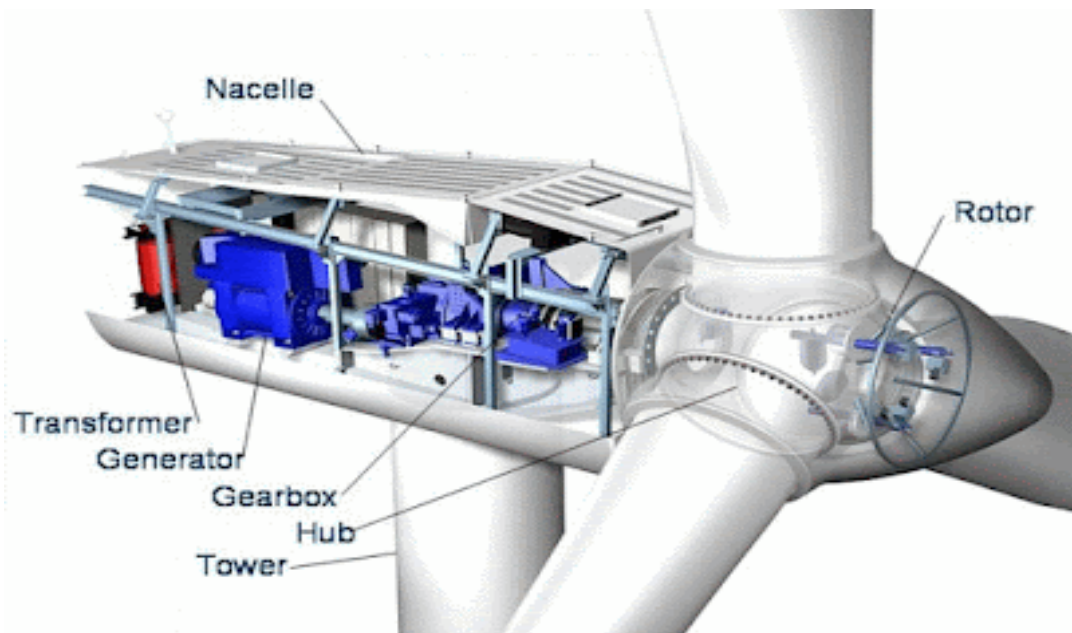


Figure 1.1. Nacelle wind turbine.

The nacelle, including the hub, rotor, gearbox, generator, inverters, hydraulics, and bearings. The nacelle is home to around 1,500 unique parts, including both big and tiny subsystems that are difficult to source separately. The kinetic energy of the wind

is converted into mechanical energy by components housed within the turbine's nacelle, which then turns a generator to produce electricity. The nacelle erected on top of the steel or concrete tower gives utility-scale machines an imposing appearance from a distance, but up close, their sheer size becomes clear. Depending on the maker and the output power, their nacelles can be over 50 feet in length and weigh 300 tons or more.

1.2. LITERATURE REVIEW

Financial viability allows the broad use of wind power as a renewable energy source. This is true not only in terms of reducing people's electricity bills, but also, and more crucially, in terms of eliminating pollution through reducing carbon emissions and other pollutants. One of wind turbines' limitations is the heat produced by the electromechanical components; unless this issue is resolved, the technology's potential for improving power output and electrical efficiency cannot be fully realized. Scientists have not ignored the heat problem throughout the last two decades, with a number of research examining how to handle the issue utilizing various existing cooling methods. Many types of research and literature studies have been carried out to cool the electromechanical equipment in nacelle wind turbine.

Nikhil Bhamare. et al., 2019 [2]. This study's objective is to identify options for enhancing the cooling of the coupling, which is a component of the power transmission system between the gearbox and the generator that heats up as a result of continuous operation. Coupling overheating activates the sensors, and the wind turbine runs in a reduced power mode to compensate for the coupling's excessive temperature increase. The program Open Foam is used to create three cases with distinct configurations. A comparative analysis is performed to determine the optimal cooling situation for coupling. The preprocessing program is Salome and the postprocessing software is Para View. This study's conclusion the bottom apertures in the nacelle cover do not aid in coupling cooling because they hinder the passage of fan2 air. And The flow rate of fan2 rises if the bottom apertures are blocked. As fan2's performance grows, this gives a greater cooling impact in the generator and coupling regions. To improve the cooling of the coupling and generator, a new

design for an enlarged fan4 duct and a 20% increase in fan4 speed have been developed.

Kadir Nuri Tekin, et al., 2014 [3]. In this study a computational approach for analyzing and characterizing the thermal behavior of a 2.5 MW wind turbine nacelle operating in cold winter conditions. At the design wind speed of 12 m/s, the effects of exterior temperatures of -30°C, -20°C, and -10 °C. on the electrical equipment and mechanical components within the nacelle have been determined. Applications for both open and closed systems have been evaluated. In both situations without air conditioning at Text=-30°C, the surface temperatures of the gearbox and generator exceed the permissible range. When the air conditioning was applied to the systems, temperatures returned to acceptable levels. For closed system applications at Text=-30 °C and -20 °C, the surface temperatures of all components are within the temperature restrictions with the capacity of the AC system, 5 kg/s at 0 °C and 5 kg/s at 10oC, despite minor icing issues within the nacelle wall. the result of this study the lowest temperature on the interior wall of the nacelle is around -14 and -10°C, causing icing issues. For the AC, 4 kg/s at 20°C, all surface temperatures are within the temperature restrictions and the minimum temperature attained on the nacelle wall is around 3 C, with no icing issues. At Text=-10oC, the surface temperatures of components with AC capacities of 4 kg/s at 30°C, 5 kg/s at 0°C, 5 kg/s at 5°C, and 5 kg/s at 10 °C are within the temperature limitations. However, in the case of the AC, 5 kg/s at 0°C, there is an issue with icing within the nacelle.

Arturo DE RISI, et al., 2014 [4]. This paper analyzes a new cooling system for wind turbines. In the proposed cooling system, the thermal load, mostly from the electrical generator, is dissipated utilizing nanofluids in the wind tower heat exchanger (WTHE). Due to their high convective heat transfer coefficient, nanofluids were shown to boost the cooling system's performance, particularly when environmental circumstances permitted the production of substantial heat fluxes. Depending on the flow rate and particle concentration, the introduction of nanofluids boosted the cooling system's efficiency by up to 30 percent under steady-state circumstances. The investigation's findings indicate that the suggested new approach is capable of ensuring extremely efficient heat transmission and limiting thermal loads on the

electrical and mechanical components of wind turbines, which are viewed as promising.

Zhou Dao, et al., 2013 [6] The objective of this study is to analyze and assess the thermal profiles of power modules cooled by air and by liquid. This study will explore and evaluate alternative cooling strategies for power modules, namely air cooling and liquid cooling, from the perspective of thermal profile evaluation. A loss profile-to-thermal-profile analysis approach for power semiconductors is proposed and proven in a multi-MW DFIG-based wind turbine system. The typical methods for air cooling and liquid cooling in wind power converters are then studied and compared with regard to the mean junction temperature and junction temperature swing. The conclusion is that the liquid cooling strategy has a similar junction temperature variation but yields a lower junction temperature mean than the air-cooling approach.

Veeresh Fuskelea. et al., 2021 [7] In the present study, the use of nanofluid to remove heat from the nacelle of a wind turbine is proposed. In this study, a 1 kW heat load on the wind turbine nacelle was investigated. Both water and Al₂O₃/water nanofluid have been subjected to numerical analysis, and their comparative findings are provided. With the use of nanofluid as a heat removal medium, heat exchange may be greatly boosted compared to water, Using the RANS-equation, this study simulated the flow of air exterior to the nacelle as well as inside the nacelle. The energy equation has been used to determine the temperature of the working fluid as a result of heat exchanges between electrical and mechanical equipment and the surrounding air. The two-equation k- model is utilized to characterize the fully developed flow in turbulent regions. The result shows an increase in the total thermal performance factor of the wind turbine.

Arezki SMAILI. et al., 2015 [8] This study examines numerically the possibility of using a clean cooling system—a magnetic refrigeration device—to cool a wind turbine nacelle that would function in a hot area (Adrar region). A hypothetical nacelle has been taken into account for this. In the computational realm, hot-plate temperature and cold-plate temperature have been used to represent, respectively, the

heat generation and the suitable cooling system idealized as isothermal conditions. A CFD approach has been used to first calculate the average air temperature within the nacelle and the necessary cooling capacity. There have been simulations run for various temperature ranges. The simulation's findings, which include the nacelle's average temperature and the necessary cooling capacity as a function of temperature span, have been collected. Next, a suitable magnetic refrigeration system has been suggested for a particular external air temperature based on the discovered cooling capacity and average air temperature within the nacelle. In comparison to traditional gas procedures, it has been shown that the prospective usage of such a device is quite promising.

M.A. Mahdi. et al., 2020 [9] The effect of turbulent natural convection heat transfer on the thermal behavior of the nacelle is currently being investigated statistically. Energy equations and Reynolds-Averaged Navier-Stokes have been taken into consideration. The resultant mathematical model has been solved using ANSYS FLUENT code. The temperature and velocity fields inside the nacelle have been presented and examined in detail as part of the results. To correctly evaluate the turbulent effect of natural convection, the resulting average temperature within the nacelle, as well as Investigating the necessary cooling capacity has led to some intriguing findings about the nacelle thermal behavior. Different cold plate temperatures have been simulated for in both 2D and 3D instances. The resulting temperature and velocity profiles within the nacelle have been shown along several axes, and they exhibit good agreement with those from the literature. A study of the 2D results was performed to determine the validity of the There has been research done on the air's temperature stratification within the nacelle. The outcome for various cooling temperatures A pleasing association between the average Nusselt number over the generator's left wall and the literature's findings were und. There has been an agreement. The 3D-case outcomes have been confirmed by illuminating the Natural convection in motion in the nacelle's cylindrical annuli. Over various radial distances, temperature profiles have been derived. directions. An adequate concordance has been found when the experimental data published in the literature are compared. The needed cooling capacity and the average temperature within the nacelle, in both 2D and 3D instances, have been taken into account in order to

estimate the effect of buoyant forces on the thermal behavior of the nacelle. According to the cooling temperature, it has been discovered that these two parameters evolve linearly. Furthermore, it has been established that correct forecasts of natural convection inside the nacelle are unquestionably necessary for determining the proper values of the needed cooling loads.

Arezki SMAILLI. et al., 2012 [10] in this research the nacelle thermal behavior of wind turbines operating in extremely hot weather is examined using a numerical technique. The Reynolds averaged Navier-Stokes equations are used to explain the air flow inside and around nacelles. Effects of heat transport have been taken into consideration using the energy equation. The governing equations that arise have been resolved using the Control-Volume Finite Element Method. Through the use of a typical commercial wind turbine, the simulations were run. The collected results, which included temperature fields in and around the nacelle, demonstrated rather logical behavior. As a function of the cold-plate temperature, the cooling capacity and temperature within the nacelle have shown linear trend fluctuations. It has also been highlighted that during nacelle thermal control, the ambient heat load makes up the majority of the contribution that must be counterbalanced by the necessary cooling capacity.

ShuIchiro Fuchino. et al., 2016 [11] In this research used a heat exchanger positioned between the stationary and rotational systems and a unique pump made specifically for the rotational system, this paper describes a method to obtain efficient heat exchange between the stationary and rotational system refrigerants for 10 MW-class superconducting generators for wind power generation. In the cooling system, the refrigerants in the stationary and rotating systems are entirely separated; a rotational-stationary heat exchanger transfers heat between the two systems. Pumps that are incredibly dependable circulate the refrigerant in rotating systems. Since there wasn't enough thrust force to reach the objective, they feel that if they increase the magnetic force and lighten the piston, the target will probably be reached. They think that the proposed cooling technique can be used with many rotating superconducting devices. They also think that by boosting the pump's capacity, superconducting power transmission cables might benefit from its use.

Mohammed Amokrane Mahdi. et al., 2013[12] in this study A typical 750 kW commercial HAWT has been used to explore the thermal behavior of electrical components inside the nacelle of wind turbines working in severe weather. For this reason, the cooling system load has been determined to be a function of the temperature within the nacelle (provided by the average temperature inside the nacelle T_{av}). In keeping with current work, it is assumed that the flow field around the turbine and nacelle, which is submerged in a uniform incoming flow parallel to the turbine's axis of rotation, is axisymmetric. A commercial CFD code the thermal behavior of the HAWT-nacelle while operating in typical high-temperature circumstances has been studied using TransAT. The code's capacity to forecast stable temperature fields inside the nacelle has been demonstrated by the preliminary findings.

M. A. MAHDI. et al., 2017 [13] The primary goal of this study is to evaluate the cooling capacity required to maintain acceptable temperature levels inside the nacelle by taking into account the buoyancy effect within the nacelle. The selected numerical technique has been validated by taking into account a hypothetical nacelle and performing a boundary layer analysis. The temperature and velocity fields inside the nacelle have been given in detail, and the results have been reviewed. Average temperature distributions within the nacelle and the necessary cooling capacity have both been looked at in order to correctly evaluate the buoyancy impact. The ensuing temperature and velocity profiles within the nacelle have been shown along several axes, and they exhibit strong qualitative agreement with the physical predictions.

A.Smaïli. et al., 2006[14] The thermal behavior of a wind turbine nacelle operating in a Nordic environment is examined numerically in this paper. The Reynolds-averaged Navier-Stokes equations are used to represent both internal airflow inside the nacelle and external airflow surrounding the nacelle and rotor. Effects of heat transport are taken into consideration by the energy equation. For the closure of time-averaged turbulent flow equations, the conventional k- ϵ model is utilized. The actuator-disk idea is used to simulate the rotor. The simulation findings proved that the air flow rate should be correctly controlled as a function of wind velocity and external air temperature in order to maintain an acceptable temperature level within

the nacelle for typical summer circumstances.

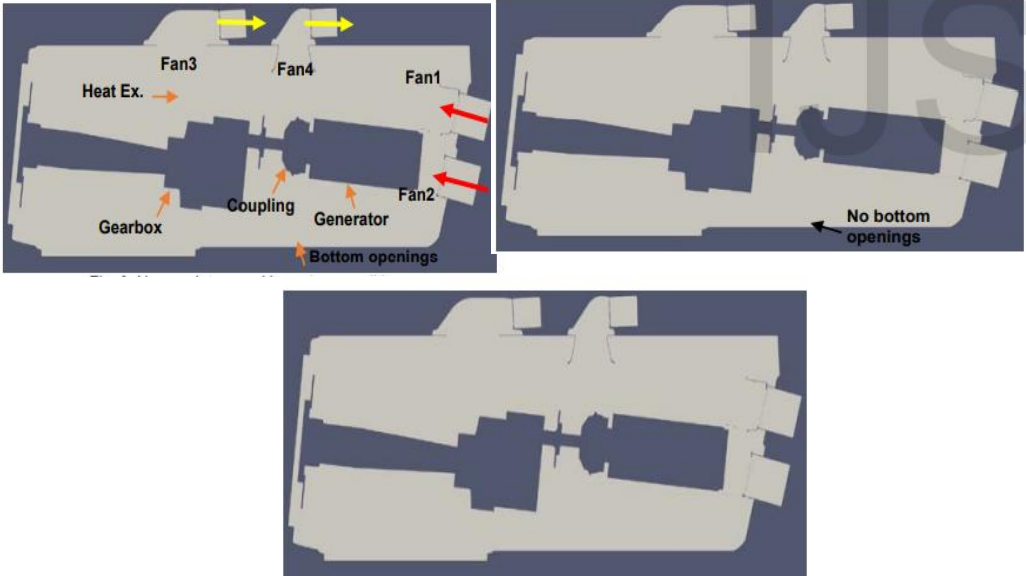
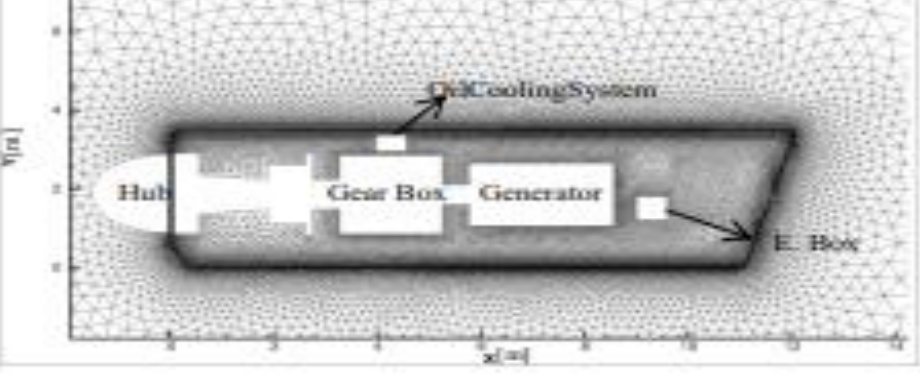
Ashwini Patel, et al., 2015[15] This research aims to determine how much the air conditioning affects the room's temperature and how much it varies. It demonstrates how the air conditioner performs in various duct placements. This study uses ANSYS Fluent to express the results of a computational fluid dynamics simulation of forced ventilation in an air-conditioned room, taking into account the occupant's thermal comfort. There are three different air conditioning room case studies considered. In case 1, we installed a single AC duct 9 feet above the ground, in case 2, we installed two AC ducts 9 feet apart with the same mass flow rate, and in case 3, we installed a split AC duct on the roof with a 9-foot separation between the two halves. Additionally, an optimized and assessed evaluation of the temperatures in Rooms 1, 2, and 3 is contained in the final results.

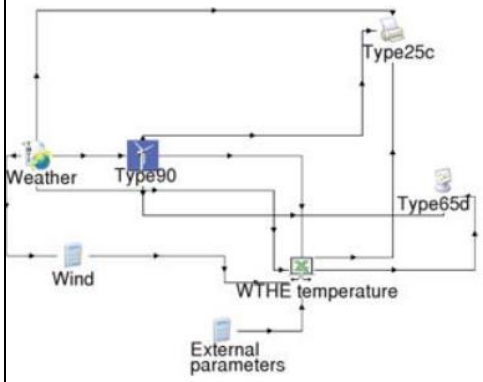
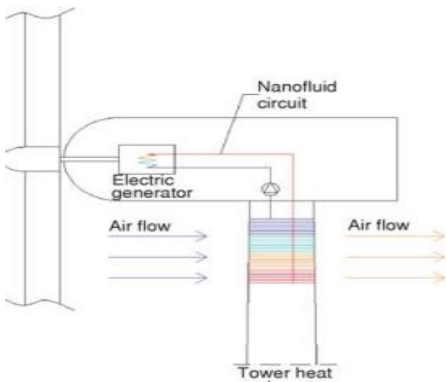
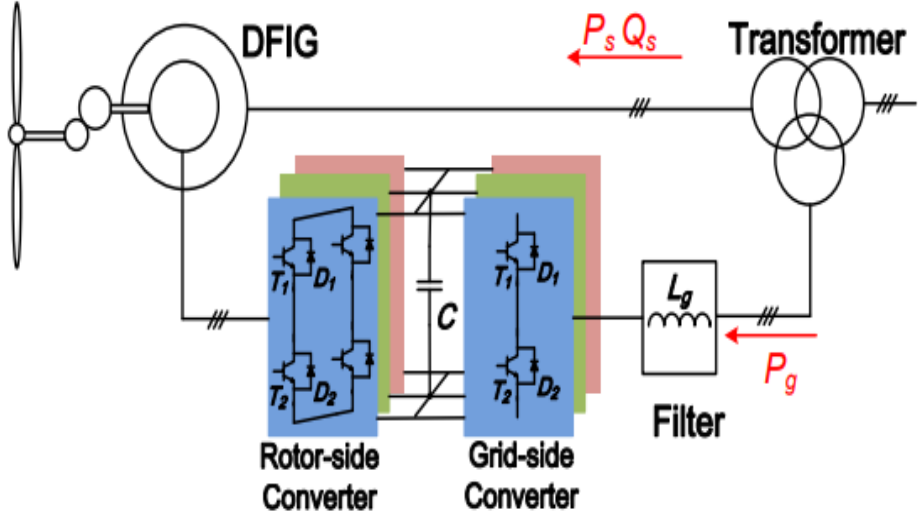
R. Pechanek et al., 2012[16] In this study, we focus on the water circulation within the housing of a water-cooled electric motor. The goal of the research is to evaluate the efficiency of two different water-cooled frame types with regard to load losses and the prevention of hot spots. The thermal load was calculated as the sum of all losses in the electrical machine. The electric motor is a recently developed electrically excited synchronous machine with applications in the automobile sector. Computational fluid dynamics were used for the creation of this piece.

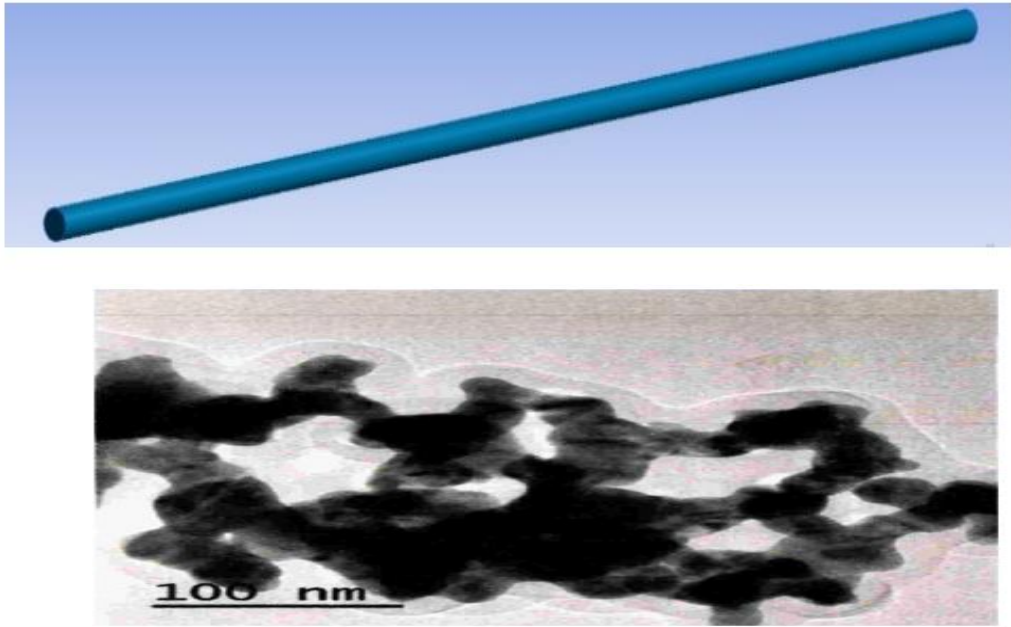
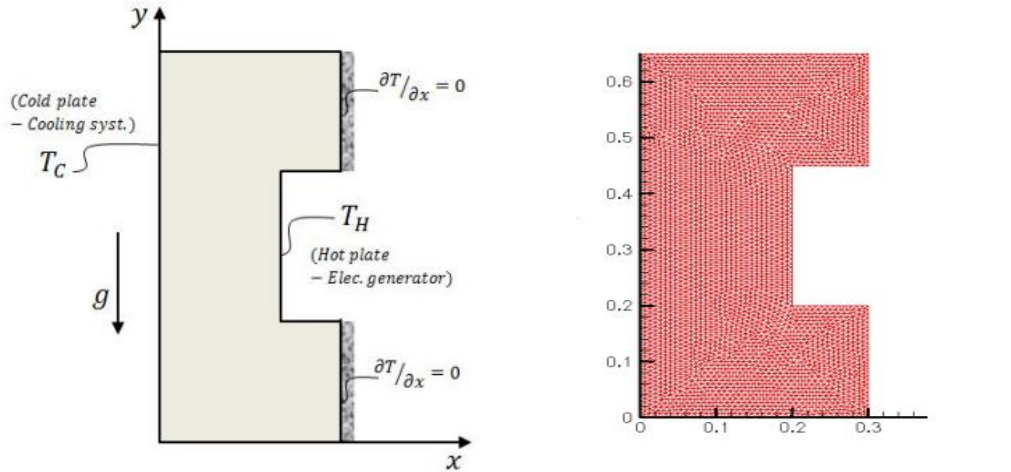
Alessandro CocliteIn, et al.2020[17] this work, multi-dimensional CFD is used to improve the efficiency of an airplane engine's cooling system. Guidelines for an effective engine design are provided by highlighting the advantages and disadvantages of various geometries. The analysis is performed using a finite-volume RANS equations solver with k-epsilon. The effectiveness of the cooling system is evaluated in relation to the inlet mass-flow rate and the cylinder jacket temperatures to account for the potential thermal effects on the engine structure. Two geometrical modifications are then recommended to increase the system's efficiency by taking into account the primary thermo-fluid dynamics properties obtained in the first configuration. Geometrical confinements and expansions of the cooling system enhance the flow characteristic loads.

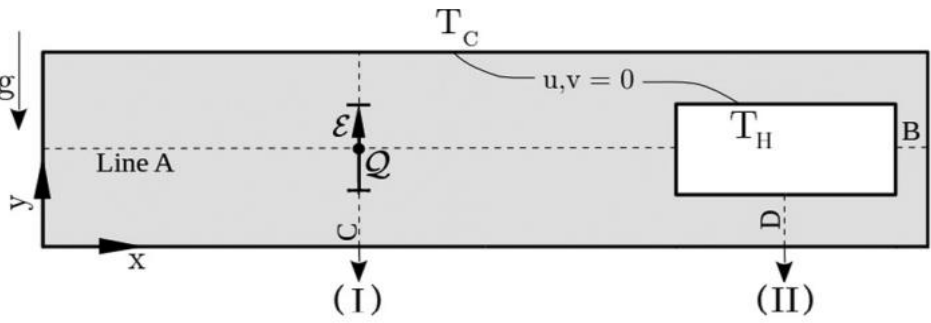
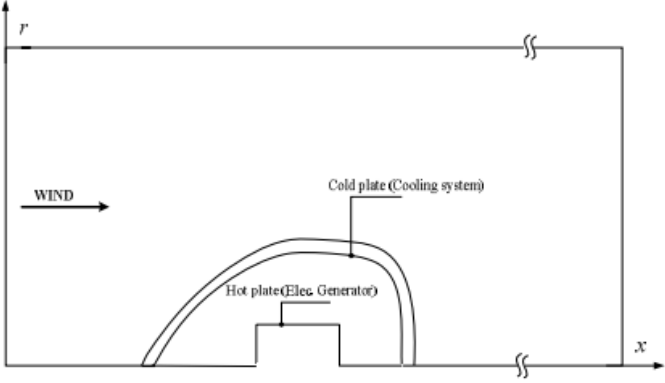
Sheng Jiana. et al., 2015[18] in this research heat load on the unit's thermal dissipation components significantly rises as wind turbine unit capacity increases. The study and development of a cooling system with high efficiency and low energy consumption become particularly vital in order to make the unit operate steadily and efficiently over the long term. The primary waste heat sources and the six basic types of cooling technologies were explained. A thorough study of each's advantages and disadvantages is also provided, and a gravity heat pipe was developed to replace the aforementioned cooling methods. This cooling method has low initial investment and low running cost, a high heat transfer efficiency, no cooling media supply equipment, and simple construction. The new technology features a simpler construction, a greater heat transfer efficiency, and reduced startup and operating expenses. Thus, the cooling system for wind turbines will utilize it extensively.

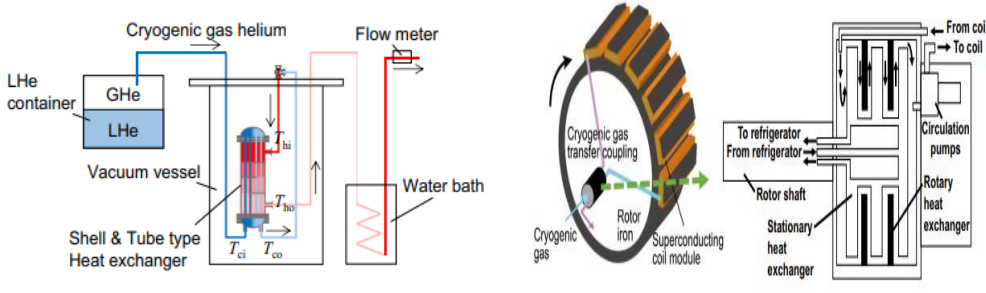
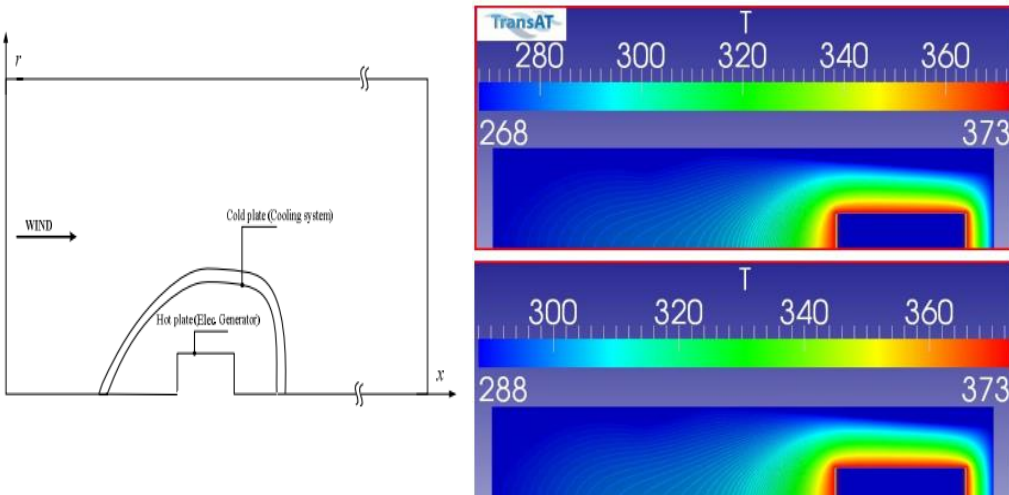
Table 1.1. Summary of the literature review.

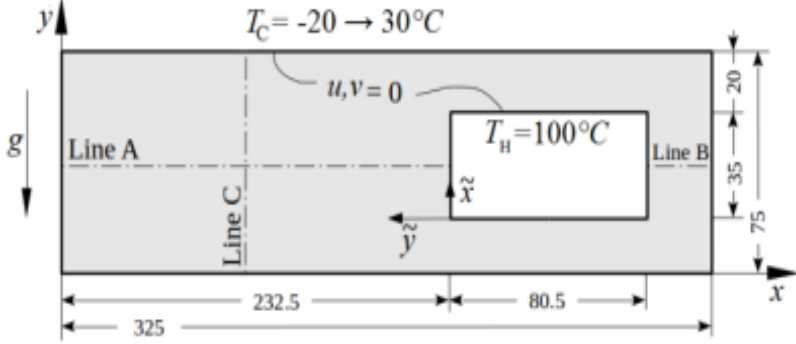
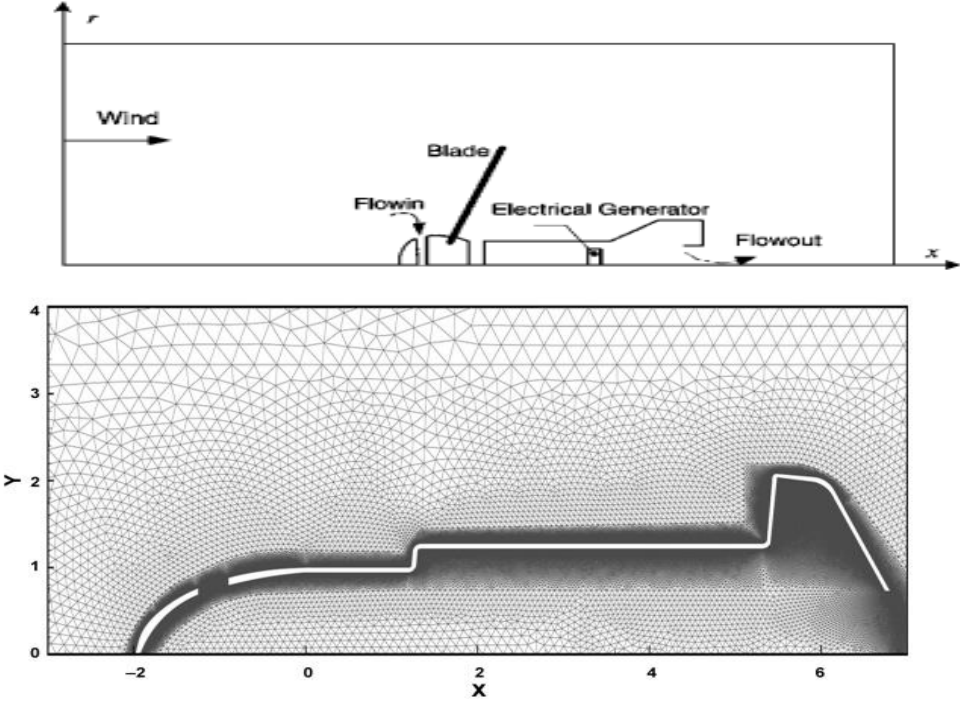
NO	Reference	Aspect studied
1	Nikhil Bhamare. et al., 2019 [2] Numerical	Case I - Baseline Case Case II with no bottom openings Case III with new duct above coupling and fan4 speed increased by 20%.
 <p>The figure displays three cross-sectional views of a nacelle. The top-left diagram shows the baseline configuration (Case I) with labels for Fan3, Fan4, Fan1, Heat Ex., Gearbox, Coupling, Generator, Fan2, and Bottom openings. Yellow arrows indicate airflow from the fans, and red arrows show flow towards the generator. The top-right diagram shows Case II, which is identical to Case I but lacks the bottom openings. The bottom diagram shows Case III, which features a new duct structure above the coupling area.</p>		
2	Kadir Nuri Tekin, et al., 2014 [3] Numerical	Geometry and unstructured grid of nacelle for CFD Analysis
 <p>The figure shows a 2D unstructured grid of a nacelle nacelle geometry. The internal components are labeled: Hub, Gear Bus, Generator, and E. Box. A Cooling System is also indicated. The grid is plotted on a coordinate system with x and y axes in meters.</p>		

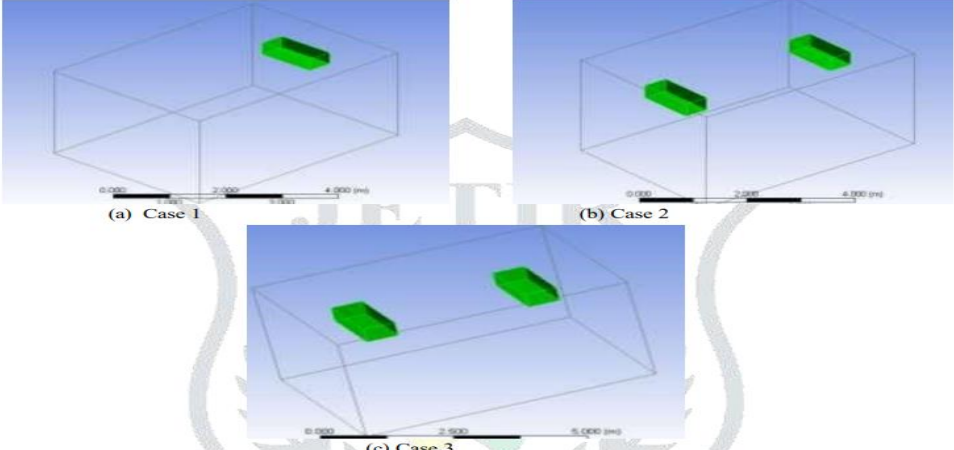
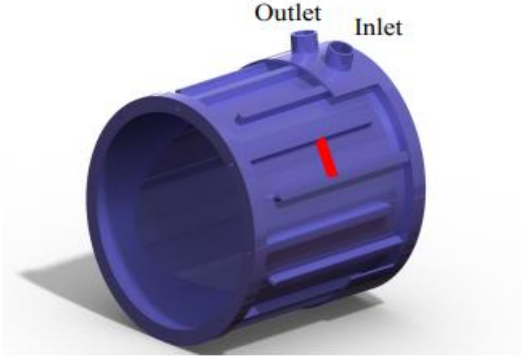
NO	Reference	Aspect studied
3	Arturo DE RISI, et al., 2014 [4] Numerical	Investigated cooling system configuration TRNSYS mode
		
4	Zhou Dao, et al., 2013 [6] Numerical	Typical configuration of a DFIG wind turbine system.
		

NO	Reference	Aspect studied
5	Veeresh Fuskelea. et al., 2021 [7] Numerical	Computational domain for the tube TEM analysis* of Al ₂ O ₃ nanoparticles
		
6	Arezki SMAILI. et al., 2015 [8] Numerical	Computational domain. Grid topology of the domain.
		

NO	Reference	Aspect studied
7	M.A. Mahdi. et al., 2020 [9] Numerical	Computational domain and boundary conditions.
		
8	Arezki SMAILa. et al., 2012 [10] Numerical	Computational domain
		

NO	Reference	Aspect studied
9	ShuIchiro Fuchino. et al., 2016 [11] Experimental	schematic of the cooling system in a superconducting generator for wind turbines. Cryogenic performance evaluation test apparatus for the heat exchanger.
		
10	Mohammed, Amokrane Mahdi. et al., 2013 [12] Numerical	Temperature field in and around the nacelle; obtained at cold-plate temperature $T_C = 268$ K, and 288 K. Computational domain
		

NO	Reference	Aspect studied
11	M. A. MAHDI. et al., 2017 [13] Numerical	Computational domain and boundary conditions.
		
12	A.Smaïli. et al., 2006[14] Numerical	Computational domain. Grid topology in the nacelle region.
		

N O	Reference	Aspect studied
13	Ashwini Patel, et al., 2015[15] Numerical	Air conditioning rooms are designed in Ansys Fluent with various duct positions.
		
14	R. Pechanek et al., 2012[16] Numerical	Frame type - with axial water flow
		

PART 2

THEORETICAL AND NUMERICAL ANALYSIS

2.1. MODELLING AND SIMULATION

An adequately modified 3D liquid Cooling system and forced air system are being used in this experiment. In accordance with the test description, a CFD model was created and tested using ANSYS FLUENT (2021).

2.1.1. Computational Fluid Dynamics (CFD)

CFD is a branch of fluid mechanics that use numerical methods and algorithms for assessing and resolving problems with fluid flow under various conditions. Computational fluid dynamics can correctly simulate flow, and heat transport, and provide some properties of complex systems with the use of computers. The advantages of CFD are summed up in reducing the length of the product design cycle, and they also give producers information for future development. Although CFD does not yield absolute results, it does enable the stimulation of several risky, expensive, trial-and-error experiments without the requirement for physical model development. CFD simulations allow for the computation of larger calculations. The CFD issue may also be displayed in more depth. The constant development of numerical algorithms and physical models is crucial for CFD as a foundational element. Finally, it is acceptable to use the CFD model as a forecasting tool in a variety of operational scenarios. The governing formulas are used in the CFD and numerically resolved to provide anticipated results based on their model finite volume. These expressions may be calculated using several turbulence modeling techniques, and they include the mass, momentum, energy, and continuity equations [19].

2.1.2. Ansys Fluent

It is a program that is used to simulate computational fluids and includes the extensive physical modeling capabilities needed in many projects. Such software has been used by many businesses all over the world as a crucial part of their manufacturing development. This software is used in wastewater treatment facilities, heat and mass transfer, and the fluid-flow model above an aircraft. This application also gains popularity because of its progressive approach, which provides quick, accurate results for computational fluid dynamics. Additionally, this application has a ton of comprehensive features, such as user-defined routines and post-processing capabilities. The last one enables the user to halt a computation and has integrated post-processing that allows users to review the results. The setup and identification of fluid and complex systems may be done easily using (ANSYS FLUENT) [19].

The processes of doing a fluid analysis are shown by the system of fluid analysis in the project diagram [20]:

- Geometry creation or import.
- Mesh generation for geometry.
- Setting up the analysis for the solver to receive Managing and overseeing the solver carrying out a solution.
- Making a report and seeing the results in a post-processor.

2.2. PROBLEM DESCRIPTION

Wind turbines must function in adverse weather, with changing temperatures throughout the day and year. Particularly, the electrical and electronic equipment inside the nacelle may experience exceptionally large temperature swings, which might result in inconsistent design stresses [21]. By rejecting to the atmosphere, the heat generated by the electrical and mechanical components as a result of various power dissipations (due to the Joule effect, friction losses released (generator, gearbox) by controlling the heat exchange between the air inside the nacelle and the air outside, the thermal effect can be managed efficiently and an acceptable

temperature inside the nacelle can be maintained. Electronics in a wind turbine nacelle face a particularly difficult challenge operating in a wide temperature range. However, effective cooling is a boon to the turbine.

2.3. DESCRIPTION OF THE PHYSICAL MODEL

2.3.1. Air Forced Cooling System

Forced air is used in this case. the generator and gearbox in the nacelle of the 1 MW turbines have been measured to be 6 m in length, 2.5 cm in width, and 3m in height [22]. There have been two fans used to pull heated air out of the nacelle and four openings used to bring fresh air inside the nacelle to cool the generator and gearbox. the surface area for the outlet was 5000cm^2 The surface area for outlet air was 315cm^2 . the air was sucked into the nacelle at three different velocities to cool the generator and gearbox. The opening for air intake and exhaust were strategically placed at the base and the top of the structure, respectively, to maximize cooling efficiency. The surface area for generator 10.064 m^2 and the surface area 3.75m^2 . Figure 2.1 illustrates more.

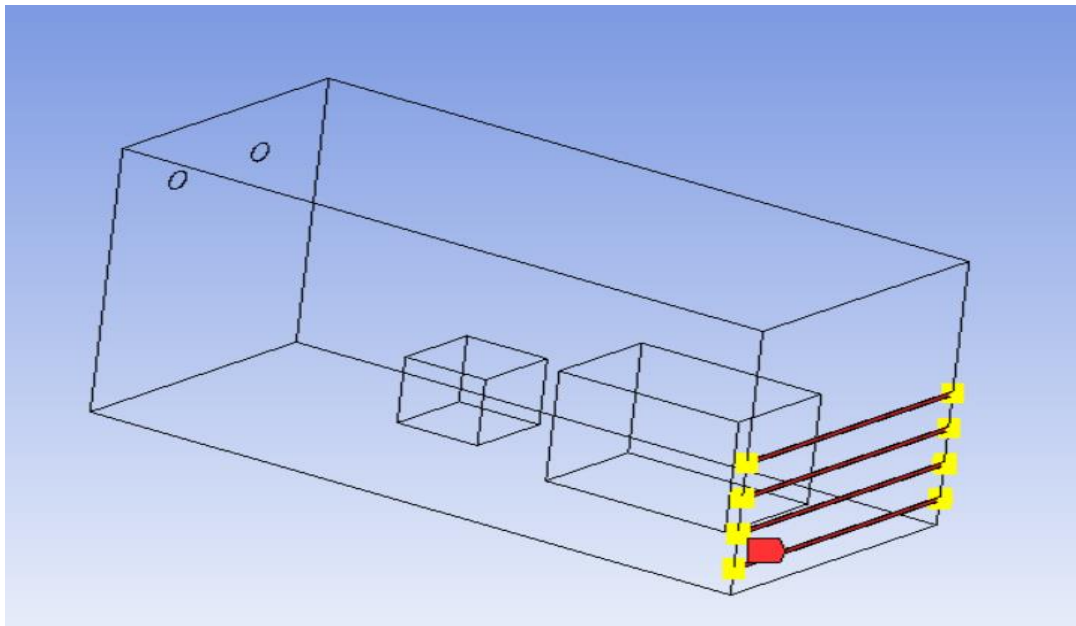


Figure 2.1. Air forced cooling system.

2.3.2. Liquid Cooling System

Cooling of the generator and gearbox, in this case, was handled by the Jet cooler. Water is admitted through three inlets and discharged through three outlets; oil is admitted through two inlets and discharged through two outlets; however, in a gearbox, only two such holes are employed. The surface area for inlet hole 58 cm^2 in generator but in gearbox the surface area 38 cm^2 . Both the air-forced system and the liquid cooling system employ the same total surface area to cool the generator and the gearbox. There were two distinct entrance temperatures employed to bring in the liquid. also depend on three different velocities for inlet water and oil.

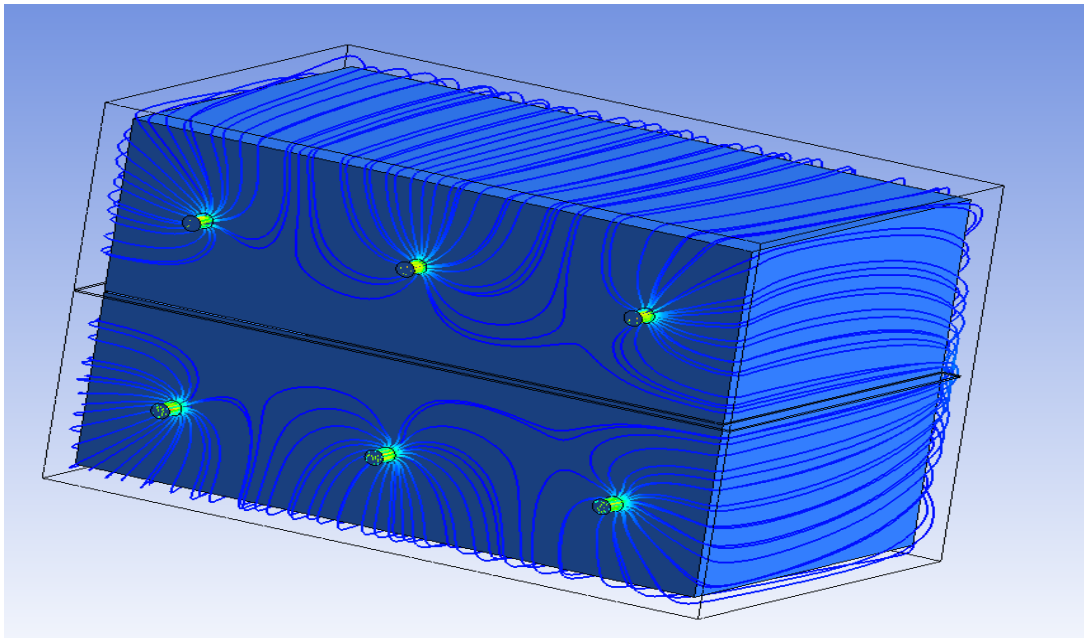


Figure 2.2. Jet cooler for generator.

2.4. ASSUMPTION AND MATERIAL PROPERTIES

- 3D and the conation are a steady state.
- In the simulations. The fluid assumes air & water and oil but the solid like the generator and gearbox assume aluminum.
- $K - \varepsilon$ stander turbulence model is used.

- The heat flux for the generator is $50 \frac{w}{m^2}$ and the heat flux for the gearbox is assumed $30 \frac{w}{m^2}$.
- The air temperature inlet is 40 and 20 °C but the liquid temperature inlet is 20 and 30 °C.
- Electromagnetic features, such as conductivity and magnetic permeability, are disregarded along with the refractive index and absorption coefficient associated with radiation.
- The inlet velocity for the air (3,5,7) m/s and the velocity for the inlet liquid (0.0005,0.001,0.0015) m/s.

Table 2.1. Property for the material.

Martial	K	Cp	ρ
Air	0.0242	1000.43	1.225
Aluminum (Generator and gearbox)	202.4	871	2719
water	998.2	4182	0.6
oil	0.30167	2900	875.9

2.5. CFD SIMULATION

The process of creating a network is crucial to the success of the simulation as a whole. The physical domain is represented by a tiny geometric structure called a grid. To apply conservation principles, it is necessary to identify the sizes of the individual components, and this is where the grid comes in. This is the first phase, and it involves doing things like generating a grid and finding the numerical solutions to equations that describe the physical process. The success of the solution depends on the accuracy of the mesh. A good mesh can be constructed by improving the quality of the solution, whereas employing a grid that is not properly developed results in discrepancies with the numerical solution. The primary building blocks in 3D are the triangular prism, the hexahedron, the tetrahedron, and the quadrilateral pyramid. These too-flexible elements are used to map mesh cells to the boundary

surface and distribute flow to other regions [23]. Sub-3D designs were created in Ansys fluent. Table 2.2 and Table 2.3 summarizes the meshing options used. The two geometries for the air-cooling system and liquid cooling system were shown in a mesh format in Figures 2.3 and figure 2.4.

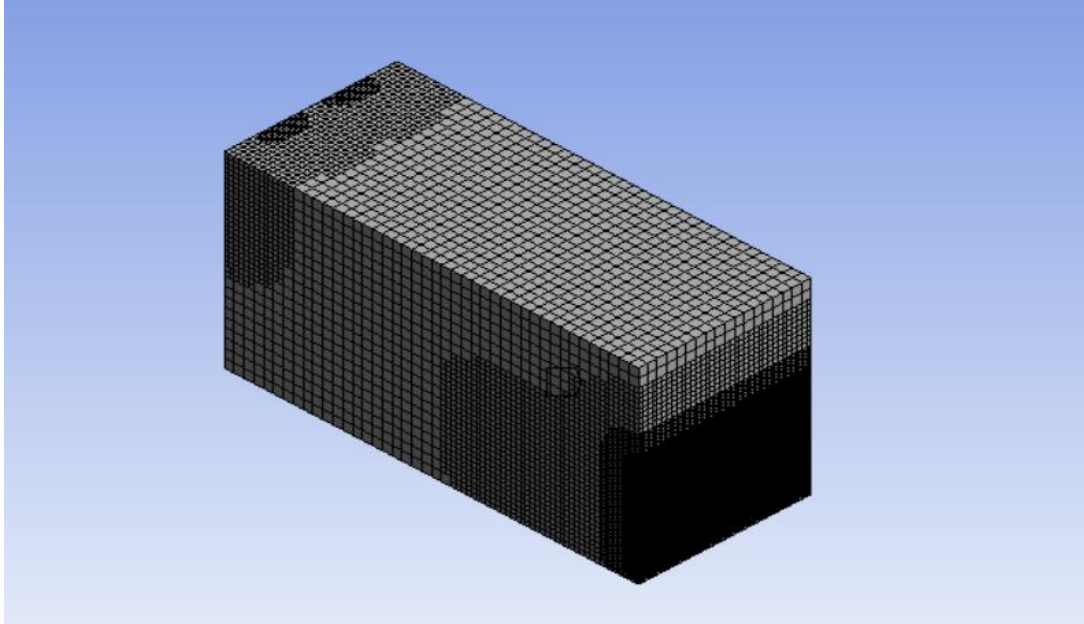


Figure 2.3. View mesh for air cooling system.

Table 2.2. Mesh-applied option for geometry in air cooling system.

Physics Reference	CFD	
Sizing		
	Size Function	Proximity and curvature
	Relevance Center	Fine
	Initial Size Seed	Active assembly
	Smoothing	Medium
	Transition	Slow
	Span Angle Center	Fine
	Max. Size	716.23 mm
	Proximity Min. Size	5.59mm
	Defeature Size	1.0 mm
Inflation		
	Inflation Option	Smooth transition
	Transition Ratio	0.272
	Maximum Layers	5
	Growth Rate	1.2

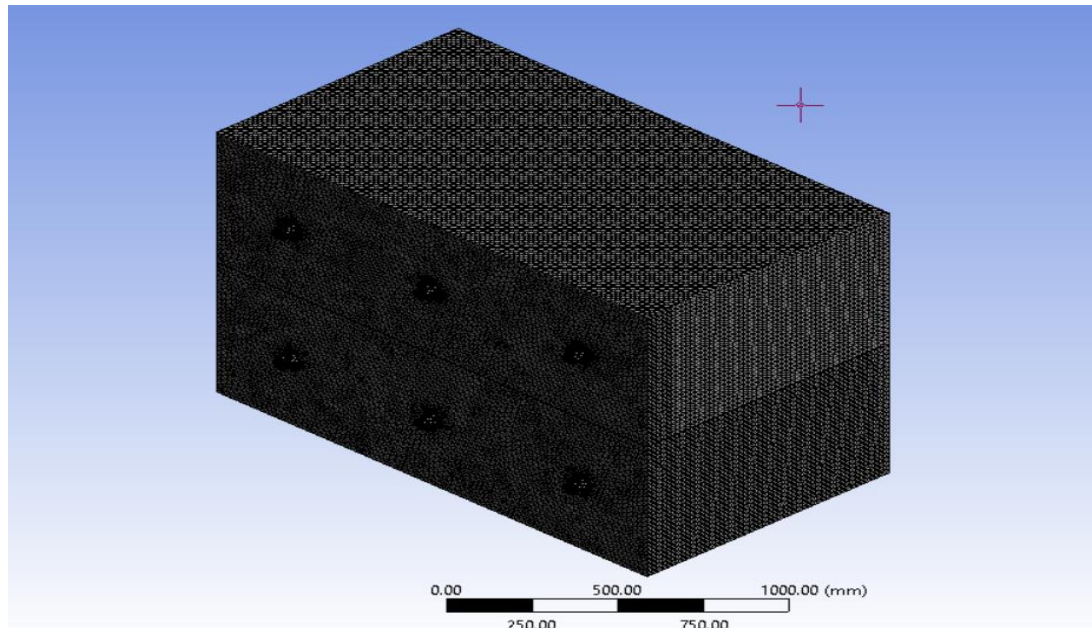


Figure 2.4. View mesh for liquid cooling system.

Table 2.3. Mish-applied option for geometry in the liquid cooling system.

Physics Reference	CFD	
Sizing		
	Size Function	Proximity and curvature
	Relevance Center	Fine
	Initial Size Seed	Active assembly
	Smoothing	Medium
	Transition	Slow
	Span Angle Center	Fine
	Min. Size	0.2 mm
	Max. Tet Size	20mm
	Defeature Size	1.0 mm
Inflation		
	Inflation Option	Smooth transition
	Transition Ratio	0.272
	Maximum Layers	5
	Growth Rate	1.2

Table (2.4) shows the results when the amount of grid elements is changed for both the air and liquid cooling systems.

Table 2.4. The impact of grid element size on the data obtained.

	Air cooling system	Liquid cooling system
Nodes	1270897	106875
Elements	1117209	485662
Metrics	Skewness	Skewness
Min.	1.3057e-010	6.7855e-004
Max.	0.64137	0.88397
Average	1.239e-002	0.22558

The numerical values representing the attributes of the materials employed in the simulation process can be found in table No. 2-1.

2.6. GOVERNING EQUATIONS

Under the primary consideration of a three-dimensional turbulent flow, a mathematical model of the governing equations of the air-forced cooling system and liquid cooling system was developed and evaluated. Non-compressible flow. has been used in CFD software to solve the Navier-Stokes equations (NSEs) in cartesian coordinate (x, y, z) for the air and cylindrical coordinate for liquid (r, θ , z) including its continuity, momentum, and energy. Thermodynamics allows us to describe the total system heat, which is used in the thermal equilibrium equation of a wind turbine cooling system [24].

1-Conservation of continuity equation in cartesian coordinate (x, y, z) [25]:

$$\frac{\partial u}{\partial x} + \frac{\partial v}{\partial y} + \frac{\partial w}{\partial z} = 0 \quad (2.1)$$

u velocity in the X direction, v velocity in the Y direction, w velocity in the Z direction.

2-Momentum equation for the incomparable and steady state in cartesian coordinate (x, y, z):

X-component:

$$\rho \left(u \frac{\partial u}{\partial x} + v \frac{\partial u}{\partial y} + w \frac{\partial u}{\partial z} \right) = -\frac{\partial p}{\partial x} + u \left(\frac{\partial^2 u}{\partial x^2} + \frac{\partial^2 u}{\partial y^2} + \frac{\partial^2 u}{\partial z^2} \right) + \rho g_x \quad (2.2)$$

Y-component:

$$\rho \left(u \frac{\partial v}{\partial x} + v \frac{\partial v}{\partial y} + w \frac{\partial v}{\partial z} \right) = -\frac{\partial p}{\partial y} + v \left(\frac{\partial^2 v}{\partial x^2} + \frac{\partial^2 v}{\partial y^2} + \frac{\partial^2 v}{\partial z^2} \right) + \rho g_y \quad (2.3)$$

Z-component:

$$\rho \left(u \frac{\partial w}{\partial x} + v \frac{\partial w}{\partial y} + w \frac{\partial w}{\partial z} \right) = -\frac{\partial p}{\partial z} + w \left(\frac{\partial^2 w}{\partial x^2} + \frac{\partial^2 w}{\partial y^2} + \frac{\partial^2 w}{\partial z^2} \right) + \rho g_z \quad (2.4)$$

3-Energy equation in Cartesian Coordinate [20]:

$$\left(u \frac{\partial T}{\partial x} + v \frac{\partial T}{\partial y} + w \frac{\partial T}{\partial z} \right) = \alpha \left(u \frac{\partial^2 T}{\partial x^2} + v \frac{\partial^2 T}{\partial y^2} + w \frac{\partial^2 T}{\partial z^2} \right) \quad (2.5)$$

α is the diffusion coefficient and calculated by use $Pr = \frac{\mu}{c_p K} \dots$

4- Conservation of continuity equation in cylindrical coordinate (r, θ, z) [26]:

$$\frac{\partial v_r}{\partial r} + \frac{v_r}{r} + \frac{1}{r} \frac{\partial v_\theta}{\partial \theta} + \frac{\partial v_z}{\partial z} = 0 \quad (2.6)$$

5- Momentum equation for the incomparable and steady state in cylindrical coordinate (r, θ, z) :

r-component:

$$\rho \left(V_r \frac{\partial v_r}{\partial r} + \frac{v_\theta}{r} \frac{\partial v_r}{\partial \theta} + V_z \frac{\partial v_r}{\partial z} - \frac{v_\theta^2}{r} \right) = \rho g_r - \frac{\partial p}{\partial r} + \mu \left[\frac{\partial}{\partial r} \left(\frac{1}{r} \frac{\partial}{\partial r} (r v_r) \right) + \frac{1}{r^2} \frac{\partial^2 v_r}{\partial \theta^2} + \frac{\partial^2 v_r}{\partial z^2} - \frac{2}{r^2} \frac{\partial v_\theta}{\partial \theta} \right] \quad (2.7)$$

θ -component:

$$\rho \left(V_r \frac{\partial v_\theta}{\partial r} + \frac{v_\theta}{r} \frac{\partial v_\theta}{\partial \theta} + V_z \frac{\partial v_\theta}{\partial z} - \frac{v_r v_\theta}{r} \right) = \rho g_\theta - \frac{1}{r} \frac{\partial p}{\partial \theta} + \mu \left[\frac{\partial}{\partial r} \left(\frac{1}{r} \frac{\partial}{\partial r} (r v_\theta) \right) + \frac{1}{r^2} \frac{\partial^2 v_\theta}{\partial \theta^2} + \frac{\partial^2 v_\theta}{\partial z^2} - \frac{2}{r^2} \frac{\partial v_r}{\partial \theta} \right] \quad (2.8)$$

Z-component

$$\rho \left(V_r \frac{\partial v_z}{\partial r} + \frac{v_\theta}{r} \frac{\partial v_z}{\partial \theta} + V_z \frac{\partial v_z}{\partial z} \right) = \rho g_z - \frac{\partial p}{\partial z} + \mu \left[\frac{1}{r} \frac{\partial}{\partial r} \left(r \frac{\partial v_z}{\partial r} \right) + \frac{1}{r^2} \frac{\partial^2 v_z}{\partial \theta^2} + \frac{\partial^2 v_z}{\partial z^2} \right] \quad (2.9)$$

6-Energy equation in cylindrical coordinate:

$$\frac{1}{r} \frac{\partial}{\partial r} \left(r \frac{\partial T}{\partial r} \right) + \frac{1}{r^2} \frac{\partial}{\partial \theta} \left(r \frac{\partial T}{\partial \theta} \right) + \frac{\partial}{\partial z} \left(\frac{\partial T}{\partial z} \right) + \frac{q_v}{k} = 0 \quad (2.10)$$

7- heat transfer

$$Q = m^\circ * Cp * \Delta T \quad (2.11)$$

$$m^\circ = \rho v A \quad (2.12)$$

8- the standard ($K - \varepsilon$) model

The ($K - \varepsilon$) turbulence model [27], which combines the kinetic energy (k) and dissipation rate (ε) equations, is used to do numerical simulations of turbulent flows:

$$\frac{\partial}{\partial x} (Ku) + \frac{\partial}{\partial y} (Kv) + \frac{\partial}{\partial z} (Kw) = \frac{\partial}{\partial x} \left(\frac{v_t}{\sigma_k} \frac{\partial k}{\partial x} \right) + \frac{\partial}{\partial y} \left(\frac{v_t}{\sigma_k} \frac{\partial k}{\partial y} \right) + \frac{\partial}{\partial z} \left(\frac{v_t}{\sigma_k} \frac{\partial k}{\partial z} \right) + G - \varepsilon. \quad (2.13)$$

$$\frac{\partial}{\partial x} (\varepsilon u) + \frac{\partial}{\partial y} (\varepsilon v) + \frac{\partial}{\partial z} (\varepsilon w) = \frac{\partial}{\partial x} \left(\frac{v_t}{\sigma_\varepsilon} \frac{\partial \varepsilon}{\partial x} \right) + \frac{\partial}{\partial y} \left(\frac{v_t}{\sigma_\varepsilon} \frac{\partial \varepsilon}{\partial y} \right) + \frac{\partial}{\partial z} \left(\frac{v_t}{\sigma_\varepsilon} \frac{\partial \varepsilon}{\partial z} \right) + C_{1\varepsilon} \frac{K}{\varepsilon} G - C_{2\varepsilon} \frac{k^2}{\varepsilon} \quad (2.14)$$

$$G = \nu_t \left[2 \left(\frac{\partial u}{\partial x} \right)^2 + 2 \left(\frac{\partial v}{\partial y} \right)^2 + 2 \left(\frac{\partial w}{\partial z} \right)^2 + \left(\frac{\partial u}{\partial y} + \frac{\partial v}{\partial x} \right)^2 + \left(\frac{\partial v}{\partial z} + \frac{\partial w}{\partial y} \right)^2 + \left(\frac{\partial u}{\partial z} + \frac{\partial w}{\partial x} \right)^2 \right] \quad (2.15)$$

Table 2.5. Gives the values of the empirical constants for (k -ε) modelling.

C_μ	$C_{1\varepsilon}$	$C_{2\varepsilon}$	σ_ε	σ_k
0.09	1.44	1.92	1	1.30

PART 3

RESULT AND DISCUSSION

3.1. INTRODUCTION

Wind turbines should be built to withstand extreme weather conditions. The weather Special consideration should be given to electrical and mechanical components are situated as they may be subjected to extremely high temperatures within the nacelle gradients of temperature, resulting in a contradictory design requirement. As a result, the goal of this research is to find the best way to cool the generator and gearbox located inside the Nacelle. using computational fluid dynamics (CFD) with ANSYS-Fluent (2021- R1) software to cool mechanical and electrical equipment. The results of numerical simulation are presented in this chapter. Two degrees of temperature were measured in the forced air in hot weather equal 40 °C and in the intermediate weather equal 20 °C. Also, in the liquid used for cooling was taken an input temperature equal to 20 °C and another degree equal 30 °C. Three different velocities were recorded in inert air and liquid at each temperature.in air forced system depend on three velocities (3, 5, 7) m/s. also in liquid cooling system deepened on three velocities (0.0005 , 0.001 , 0.0015)m/s. This chapter illustrates a relationship between mass flow rate and temperature of generator and gearbox in air forced cooling system and liquid cooling system. There was also a relationship established between the total amount of heat transferred and the mass flow rate of air and liquid. This chapter also includes an inventory of the temperature distributions of the generator and the gearbox extracted from the simulation.

3.2. FORCED AIR-COOLING SYSTEM

3.2.1. Air Temperature 20 °C

Currently, there are three cases:

Case I: At an external temperature of 20 °C and a velocity of 3 m/s, Figure 1 displays the simulation results of velocity fields inside the nacelle.

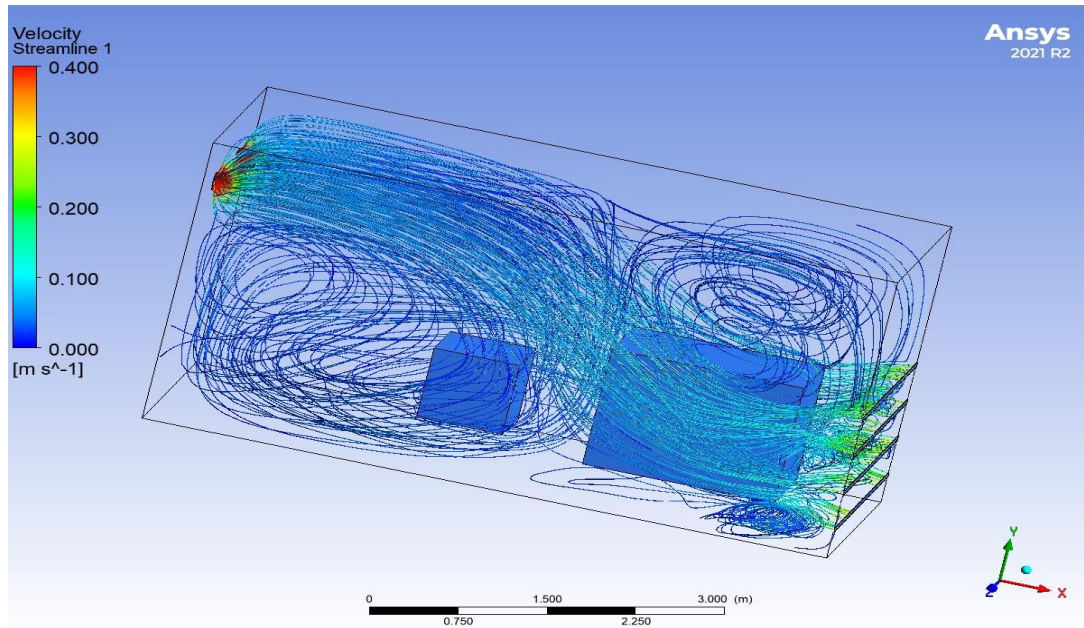


Figure 3.1. Velocity contour for 3m/s.

The simulation shows the lowest speed entered into the descendant and how the speed degree affects the temperature of the generator and the gearbox.

The temperature date obtained for generator and gear box inside nacelle after 1000 alteration:

Table 3.1. Temperature date for case I.

Generator °C	Gear box °C
65	58

The results of the temperature of the generator and the gearbox relative to the conditions we have imposed are not good but acceptable.

Case II. Figure 2 show simulation result for the velocity contour at an external temperature of 20°C and velocity 5 m/s.

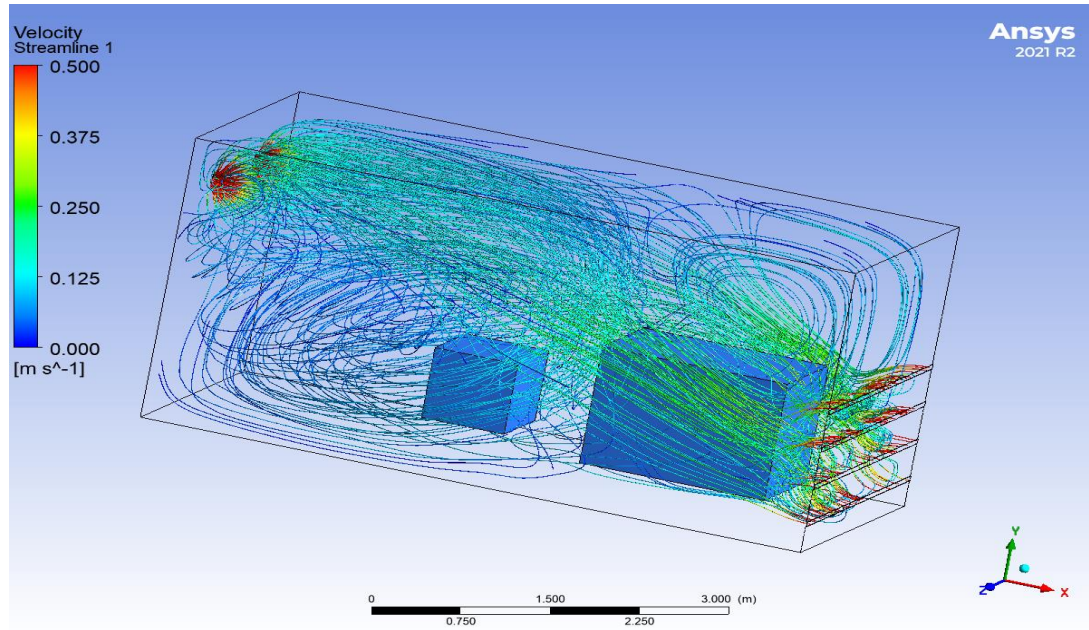


Figure 3.2. Velocity contour for 5m/s.

The simulation in this instance demonstrates how the nacelle thermal analysis is impacted by an increase in the velocity. the temperature date obtained for generator and gear box inside nacelle after 1000 alteration:

Table 3.2. Temperature date for case II.

Generator (°C)	Gearbox (°C)
49	38

The temperature of the generator and gearbox changed under identical circumstances as in the previous scenario, with the exception of accelerating air entry.

Case III. Figure 3 show simulation result for the velocity contour at an external temperature of 20°C and velocity 7 m/s.

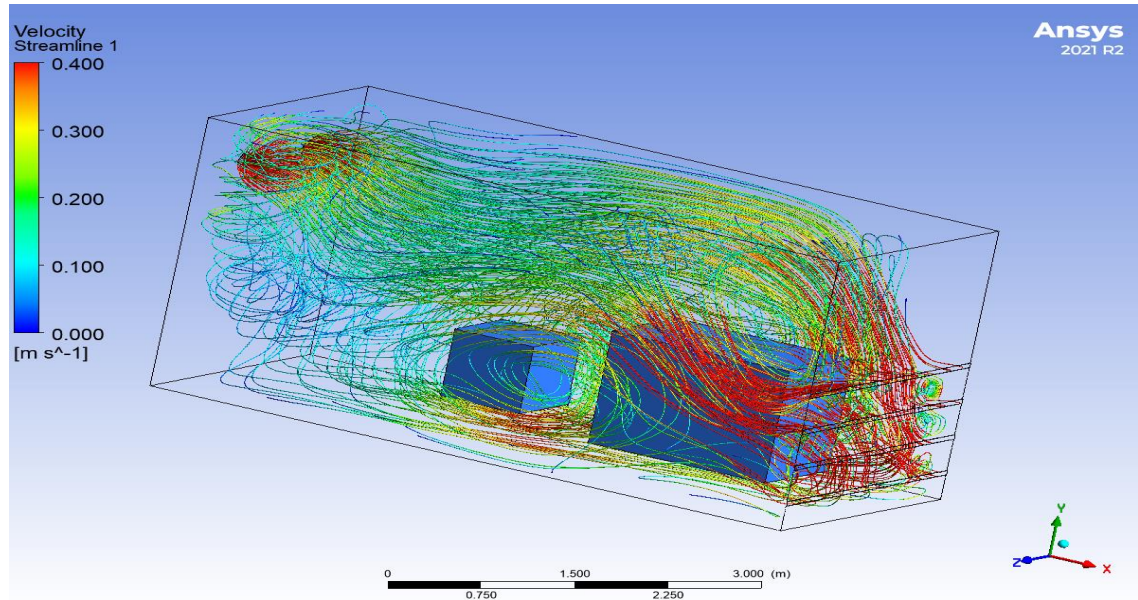


Figure 3.3. Velocity contour for 7m/s.

Due to the high speed, the simulation technique differs from the previous two scenarios and depicts the flow of outside air through the Nacelle entrance holes. The temperature data obtained for generator and gearbox inside nacelle after 1000 alteration:

Table 3.3. Temperature data for case III.

Generator (°C)	Gearbox (°C)
34	28

It has been noted that the temperature of the generator and gearbox in this case is better than in the previous two situations, demonstrating that the mass flow rate of air has a substantial impact on the temperature inside the nacelle.

Results obtained at Text= 20 °C are presented in Figure 4. For all cases.

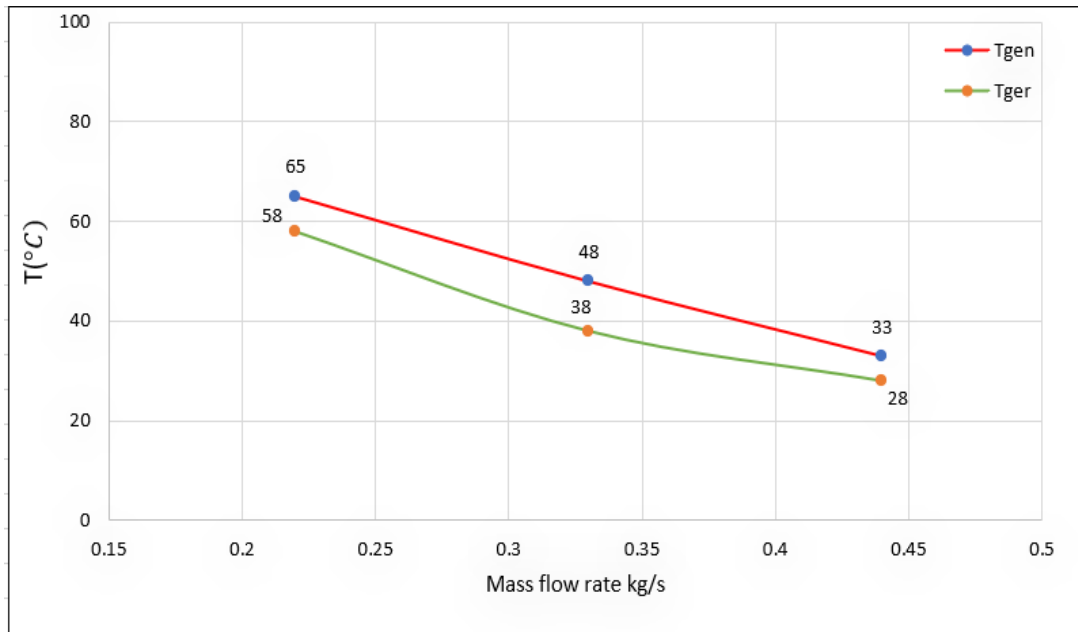


Figure 3.4. Variation of mass flow (Kg/s) rate and temperature (°C).

The red line on the y-axis shows the temperature of the generator, the green line the temperature of the gearbox, and the X axis the mass flow rate of air. The relationship of (m°) with (T) is inversely. The values of (m°) cases (1, 2, and 3) calculated as (0.22 Kg/s, 0.36 Kg/s, 0.44 Kg/s). This demonstrates that high mass flow rate decreases the temperature for the generator and gearbox.

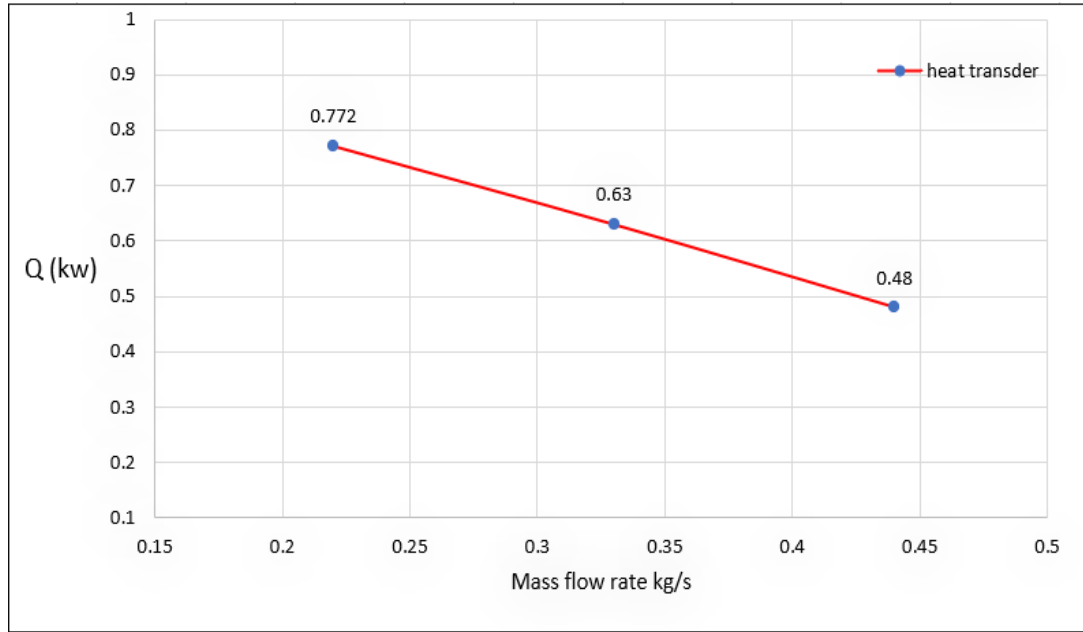


Figure 3.5. Variation of mass flow (Kg/s) rate and heat transfer (KW).

The drawing shows us that the transferred heat decreases as the mass flow rate rises. Because increasing speed does not give enough time to transfer heat. Temperature distribution according to the speed found in the simulation. have three different cases.

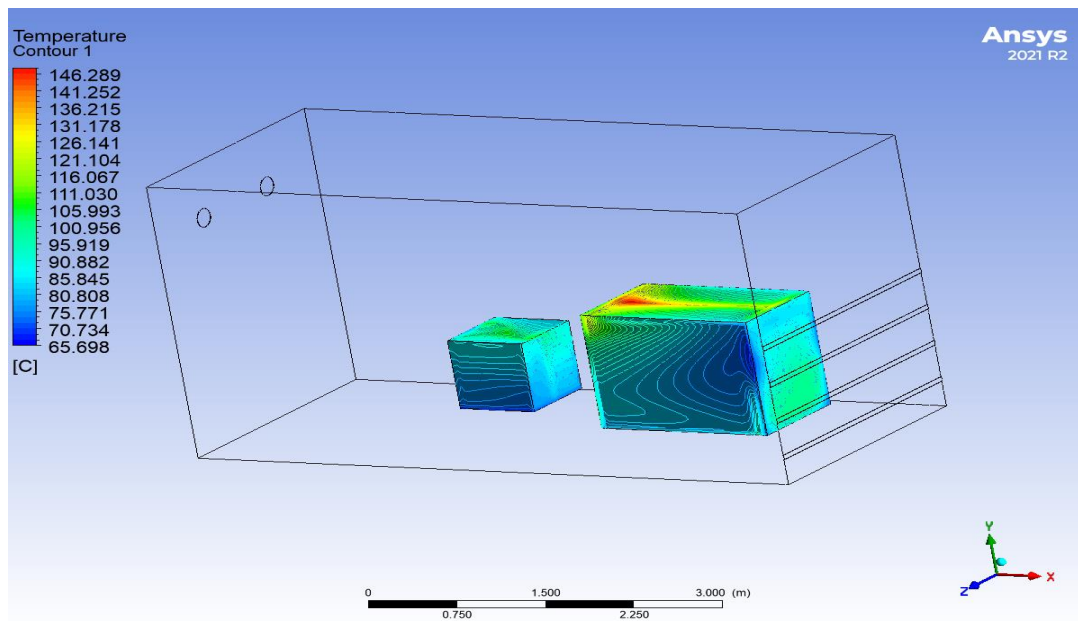


Figure 3.6. Temperature distribution for generator and gear box in 20°C for 3 m/s.

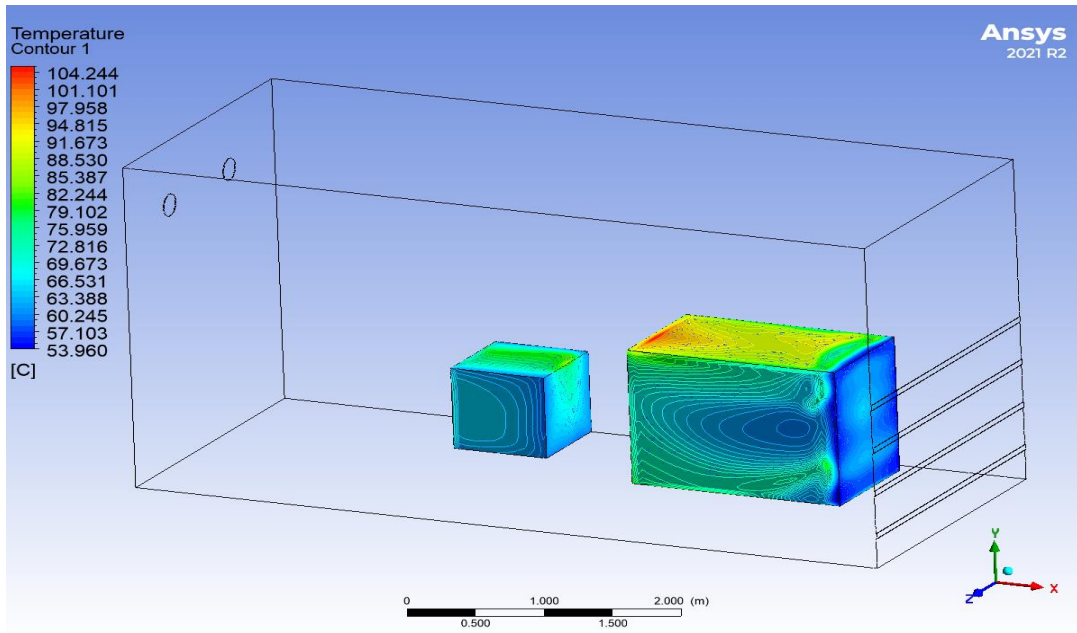


Figure 3.7. Temperature distribution for generator and gear box in 20°C for 5 m/s.

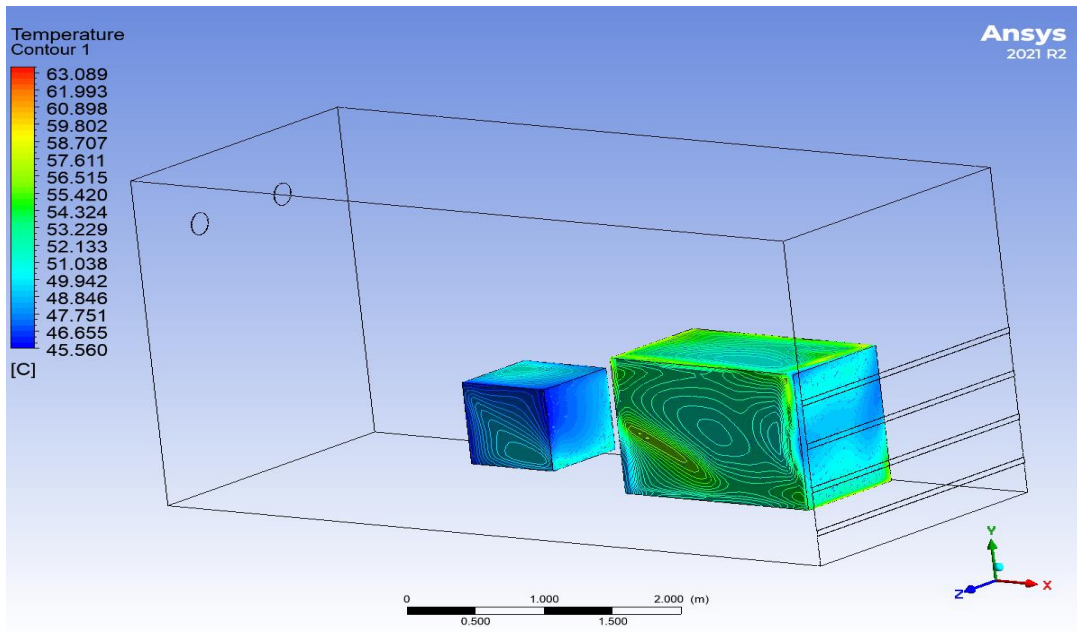


Figure 3.8. Temperature distribution for generator and gear box in 20°C for 5 m/s.

3.2.2. Air Temperature 40 °C

In this point as well, the generator and the gearbox were cooled by the use of forced air, but under 40 degree and three different velocities, so in this point have three cases.

Case I: Figure 7 shows the results of the simulation of the velocity fields inside the nacelle at an external temperature of 40 °C and a velocity of 3 m/s.

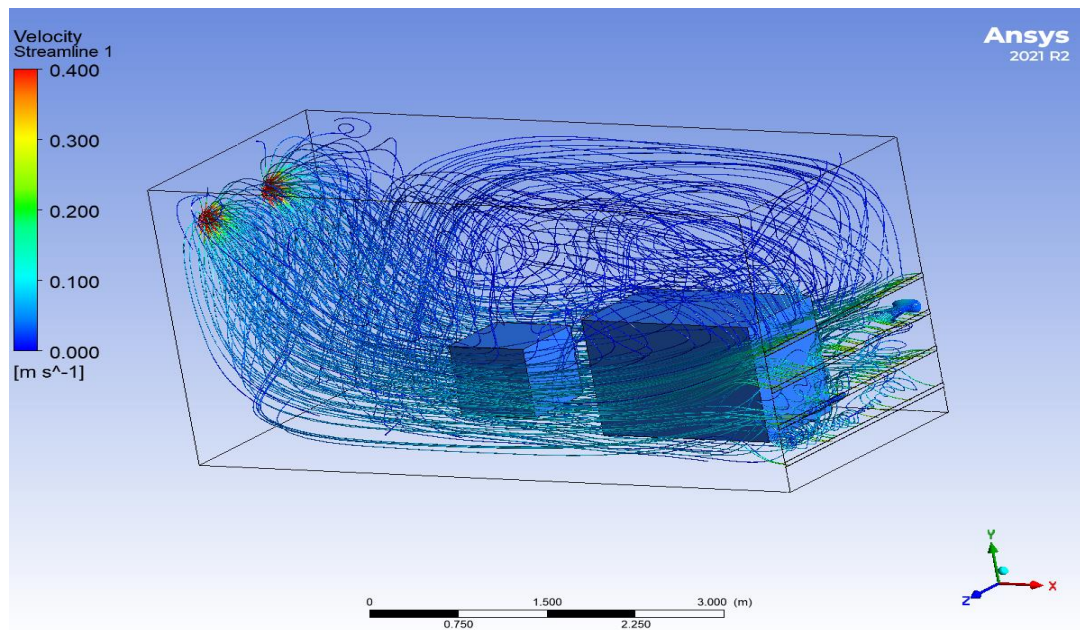


Figure 3.9. Case I velocity contour for 3m/s.

The simulation displays the descendant's lowest speed as well as how the speed degree influences the gearbox and generator's temperature. The temperature date obtained for generator and gear box inside nacelle after 1000 alteration:

Table 3.4. Temperature date for case I.

Generator (°C)	Gearbox (°C)
85	79

The method of using air to cool at high temperatures with low speed can harm the mechanical and electrical components in the nacelle since this situation is extremely

severe compared to other cases. Therefore, such a method is considered unsuccessful according to the numbers obtained from the simulation.

Case II: Figure 8 displays the velocity contour simulation results with a 40°C ambient temperature and 5 m/s velocity.

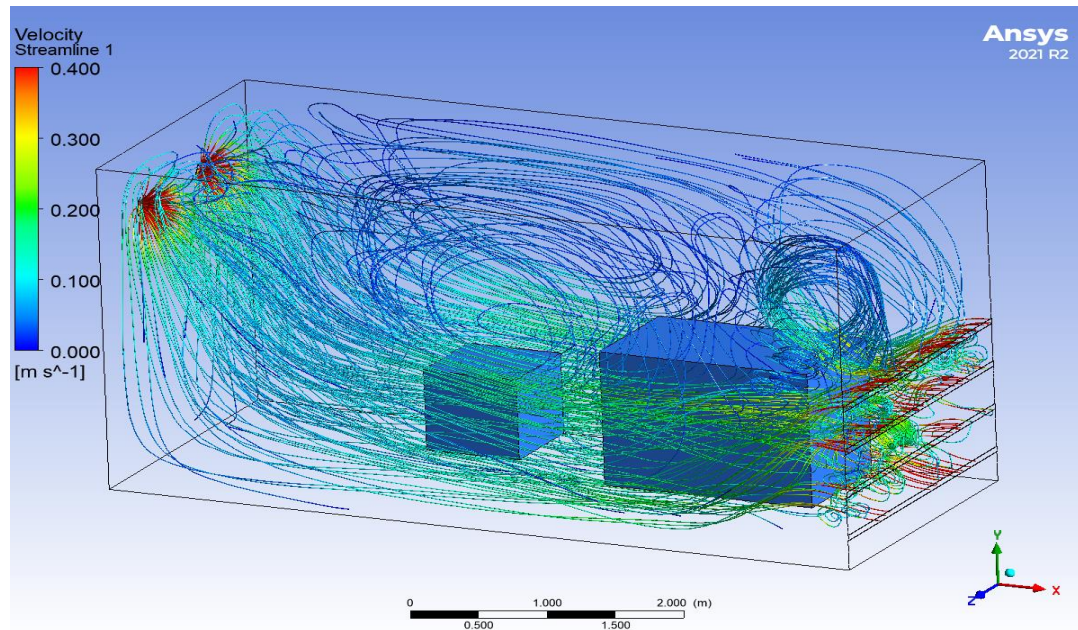


Figure 3.10. Velocity contour for 5m/s.

The temperature data obtained for generator and gear box inside nacelle after 1000 alteration:

Table 3.5. Temperature data for case II.

Generator (°C)	Gearbox (°C)
68	58.5

With an increase in entry speed, it was discovered that the temperature had improved from the prior instance. However, given the high temperature of the atmosphere, the cooling system for the generator and gearbox was inadequate, and a more effective cooling system had to be designed. The temperature data obtained for generator and gear box inside nacelle after 1000 alteration:

Case III. Figure 9 show simulation result for the velocity contour at an external temperature of 40°C and velocity 7 m/s.

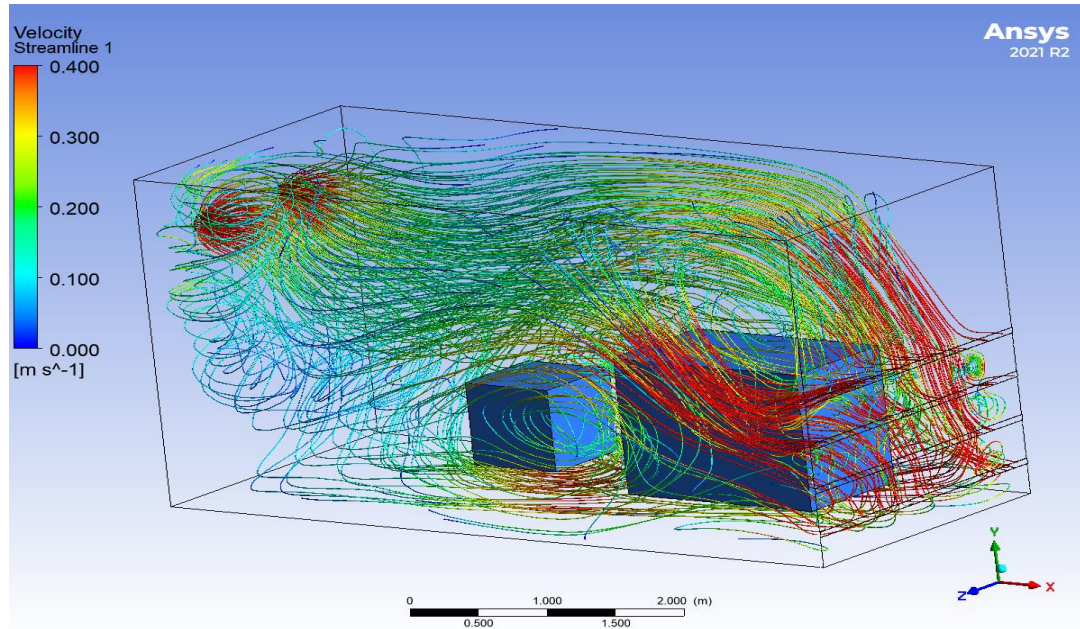


Figure 3.11. Velocity contour for 7m/s.

Simulations with the same weather circumstances as before employed the greatest air speed. The simulation demonstrates that the cooling process is strongly impacted by the entry process. The temperature data obtained for generator and gear box inside nacelle after 1000 alteration:

Table 3.6. Temperature data for case III.

Generator (°C)	Gearbox (°C)
53	48

Compared to the other two cases, a significant improvement was seen in this instance. Future use of these containers can be enhanced by regulating the entry temperature and achieving greater cooling of mechanical and electrical components. A diagram was created between the mass flow rate of air and the temperature of the nacella component parts in order to clearly depict what was occurring. Results obtained at Text= 40°C are presented in Figure (3-10) For all cases,

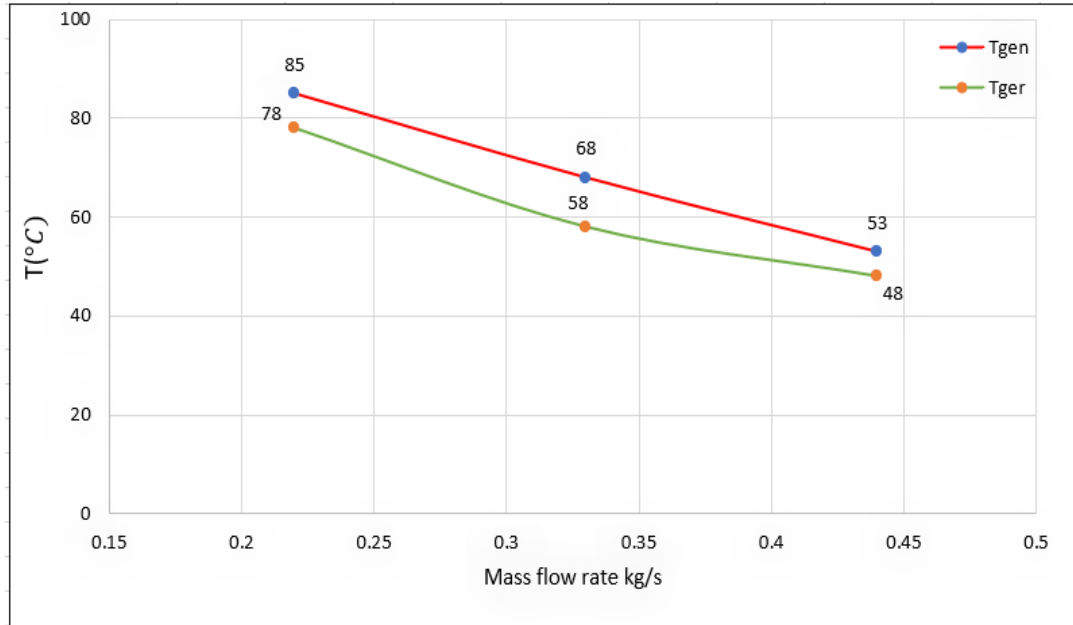


Figure 3.12. Variation of mass flow (Kg/s) rate and temperature (°C).

The relationship between temperature and mass flow rate The mass flow rate in the system is inversely proportional to the temperature in the system, as we have already discussed. That is, the temperature gets smaller as the mass flow rate gets more. Therefore, it was found that the temperature of the gearbox and generator corresponds in the opposite direction to the flow process.

Additionally in fig11, a correlation was drawn between the mass flow rate and the amount of heat transported. The relationship has shown that the highest quantity of heat is removed when the velocity of the air decrease. Where the mass flow rate and the amount of heat transported are theoretically computed

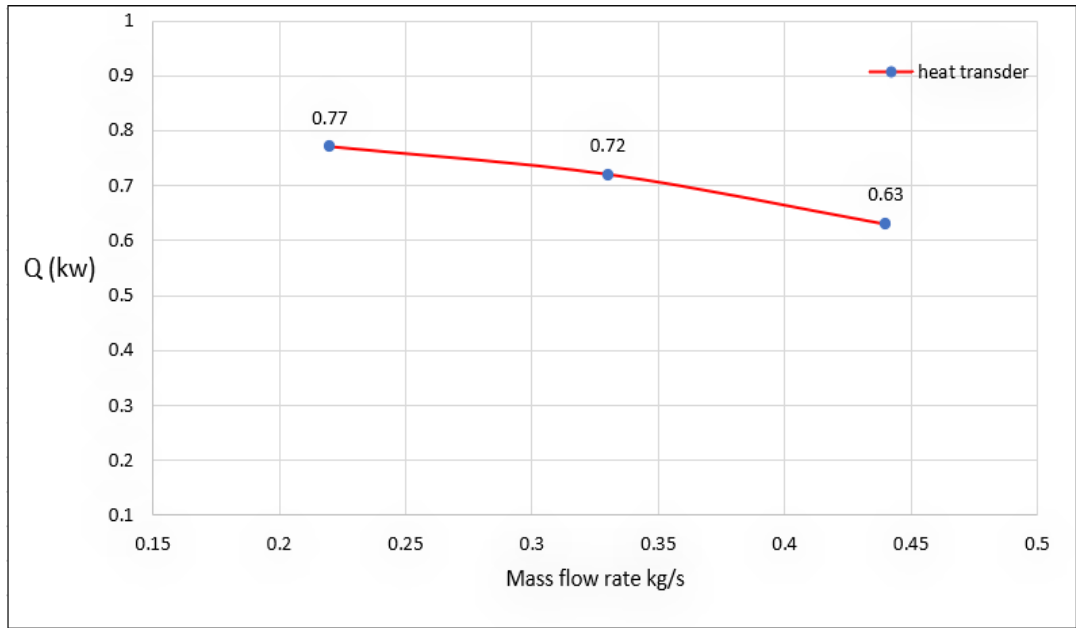


Figure 3.13. Variation of mass flow (Kg/s) rate and heat transfer (KW).

In figure (4-12) the gearbox and generator's temperature distribution throughout the previous three situations. where there is a little variation in the mechanical and electrical components' thermal analysis.

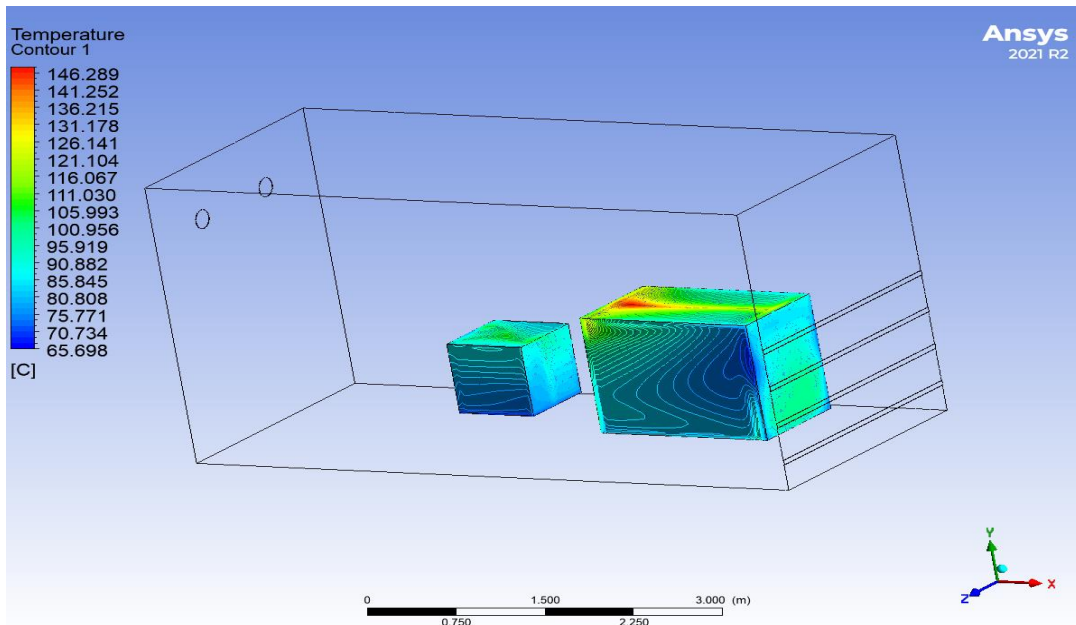


Figure 3.14. Temperature distribution for generator and gear box in 3m/s.

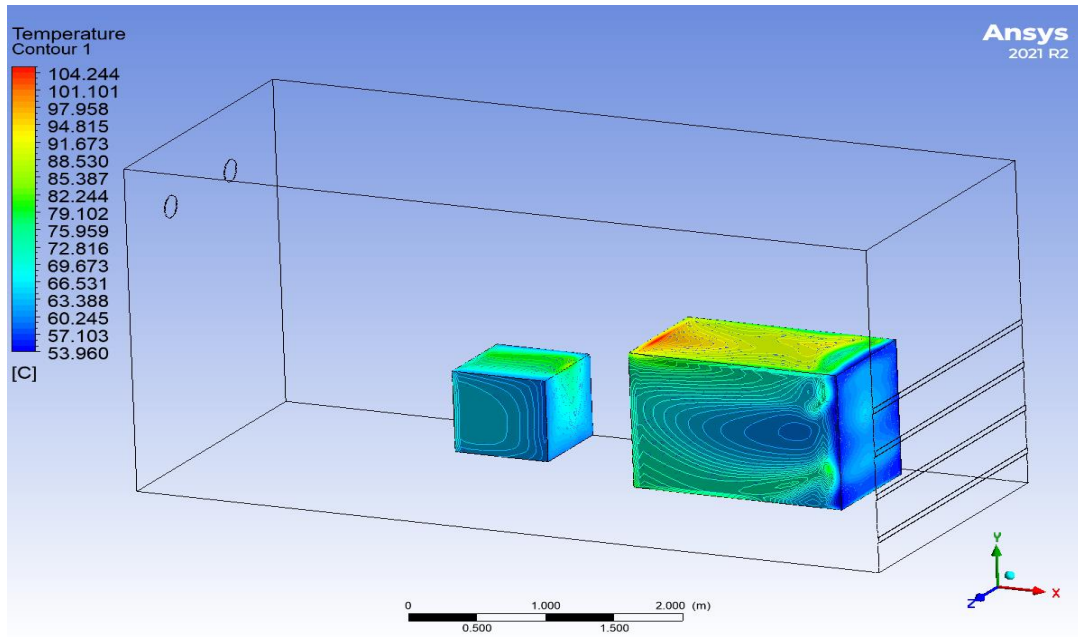


Figure 3.15. Temperature distribution for generator and gear box in 5m/s.

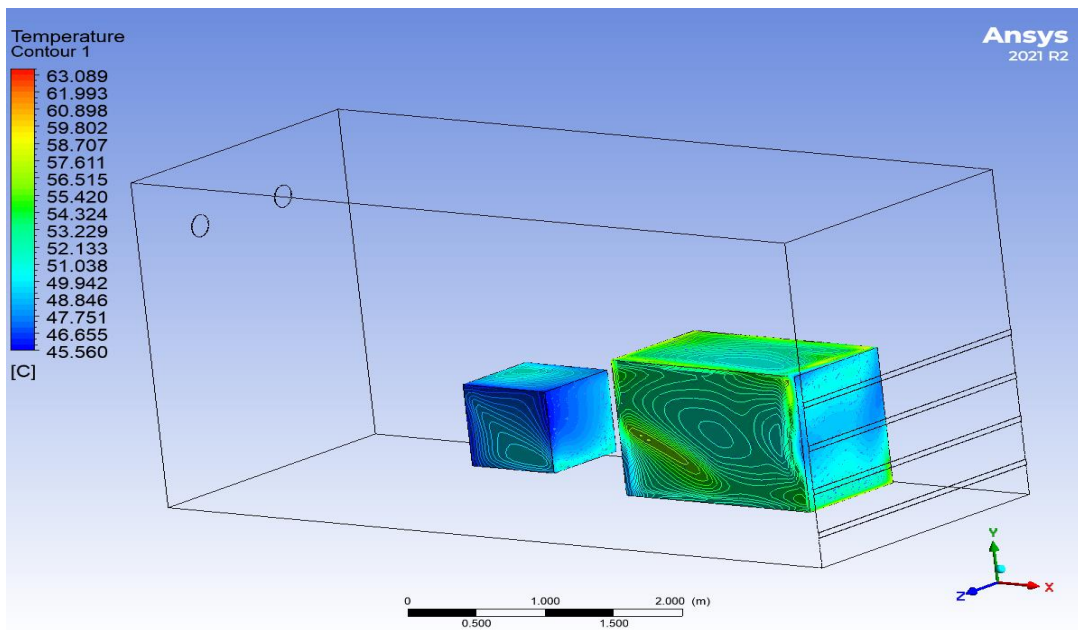


Figure 3.16. Temperature distribution for generator and gear box in 7m/s.

3.3. LIQUID COOLING SYSTEM

The problem of poor cooling output and the huge size of the air cooling system can be resolved by the liquid medium's significantly greater cooling capabilities and more compact system layout. Liquid cooling systems for the gearbox and generator

have been simulated in six cases. As much cooling as possible was obtained from the mechanical and electrical parts of the nacelle by using water to cool the generator and oil to cool the gearbox, as well as two entrance temperatures and three different speeds.

3.3.1. Liquid Temperature 20 °C

After performing the simulation of three different velocities for water and oil. the following temperature results were obtained:

Table 3.7. Temperature data for liquid cooling system in 20 °C.

Velocity m/s	Gearbox (°C)	Genertor(°C)
0.0005	29	41
0.001	25	31
0.0015	24	28

Through the temperature readings obtained through the simulation, it was found that the cooling with the liquid obtained is good compared to the cooling with forced air. Additionally, it has been noted that the temperature of mechanical and electrical components is significantly influenced by the flow rate of water or oil. Where we notice that when the speed of entry of the liquid increases, the temperature decreases. To further demonstrate this, a correlation between the temperature generated following cooling and the mass flow rate that was theoretically deduced from the available data was drawn in figure13 & 14. A relationship was also drawn between the transferred heat and the mass flow rate of the liquid in figure15&16. It was observed that the greater the flow process, the greater the amount of heat from the mechanical and electrical components.

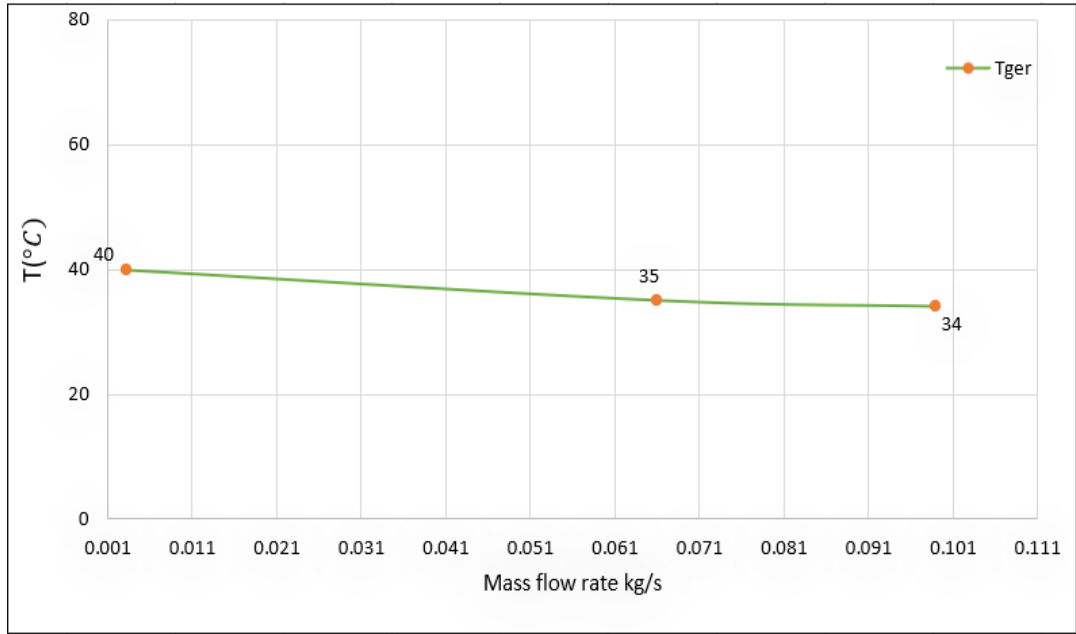


Figure 3.17. Variation of mass flow (Kg/s) rate and temperature for the gearbox (°C).

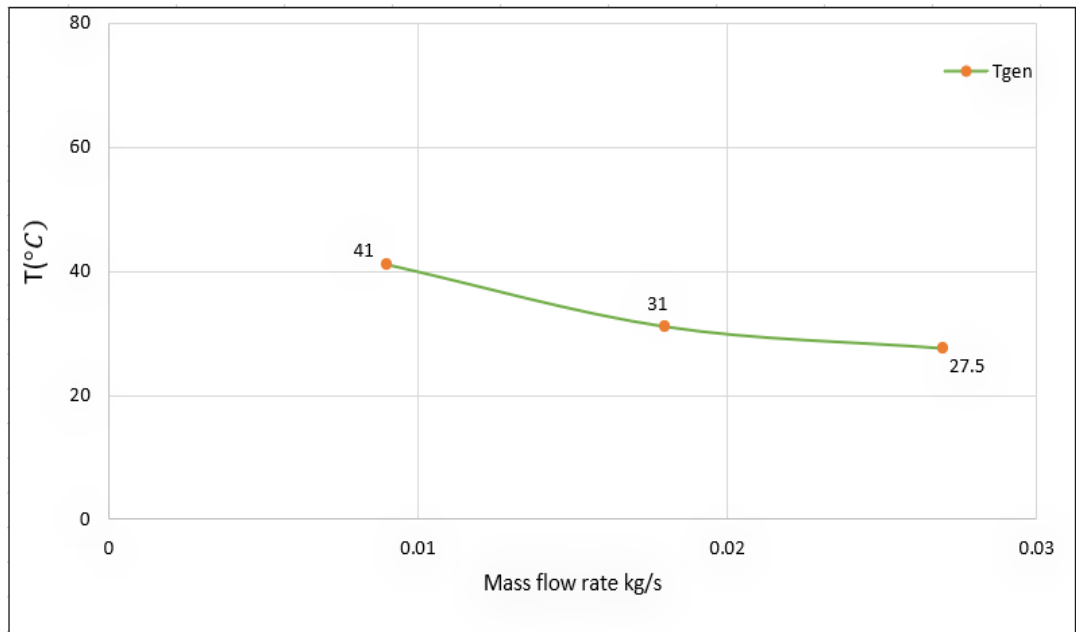


Figure 3.18. Variation of mass flow rate (Kg/s) and temperature for generator (°C).

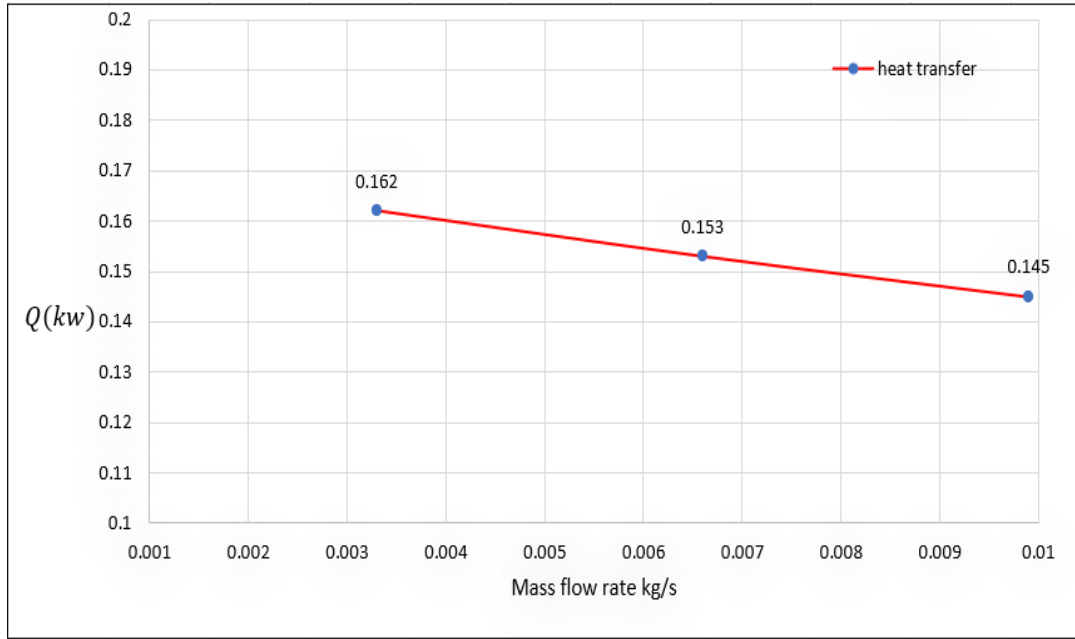


Figure 3.19. Variation of mass flow rate (Kg/s) for oil and heat transfer (kw).

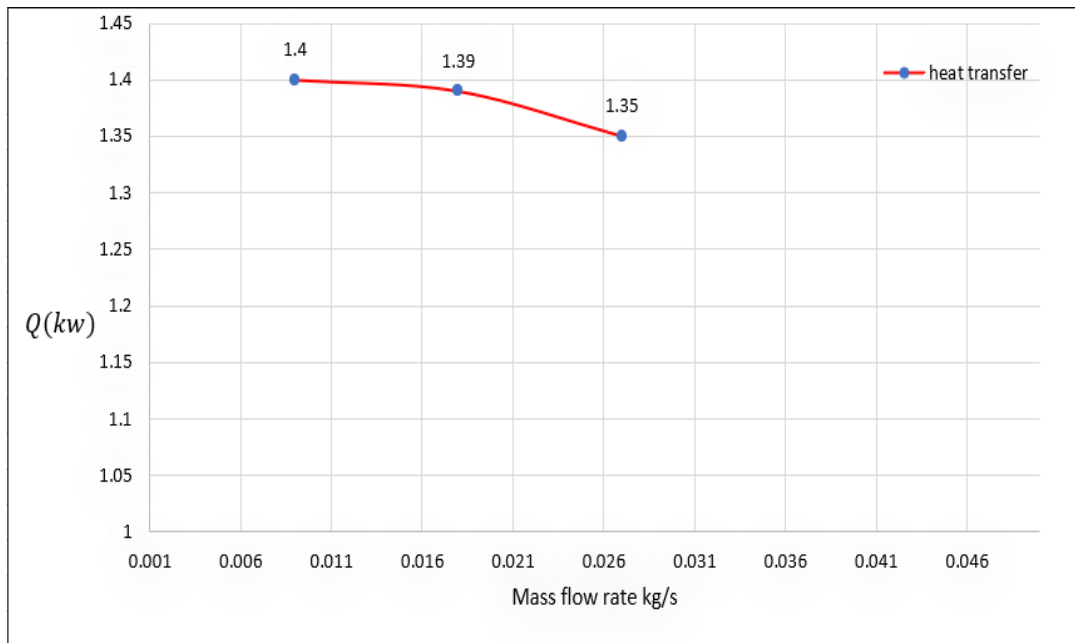


Figure 3.20. Variation of mass flow rate (Kg/s) for water and heat transfer (kw).

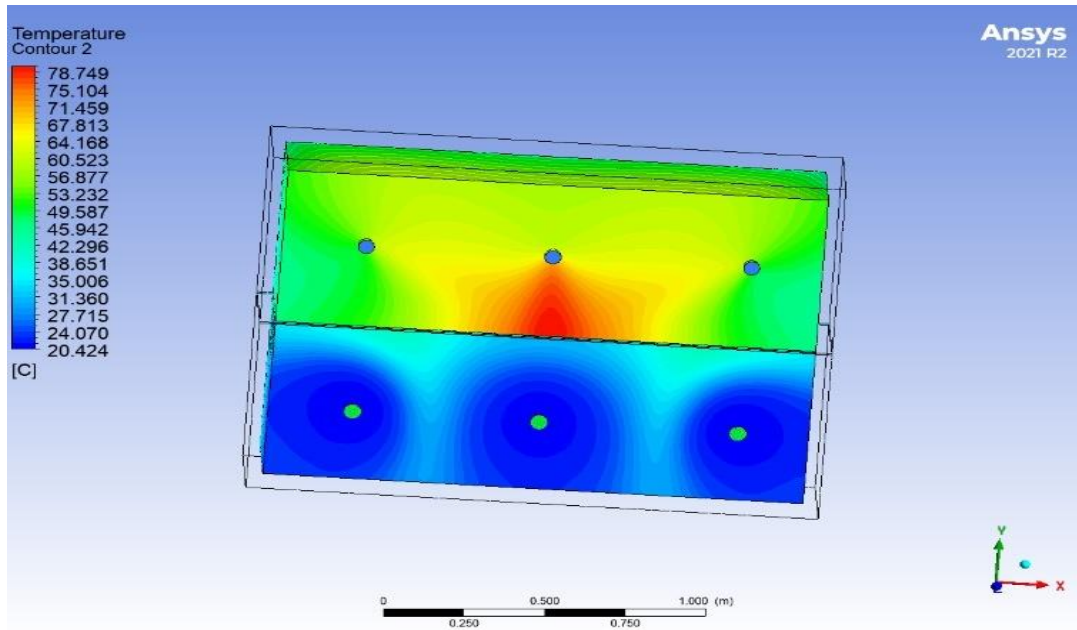


Figure 3.21. Temperature distribution for generator in 20°C in 0.0005m/s.

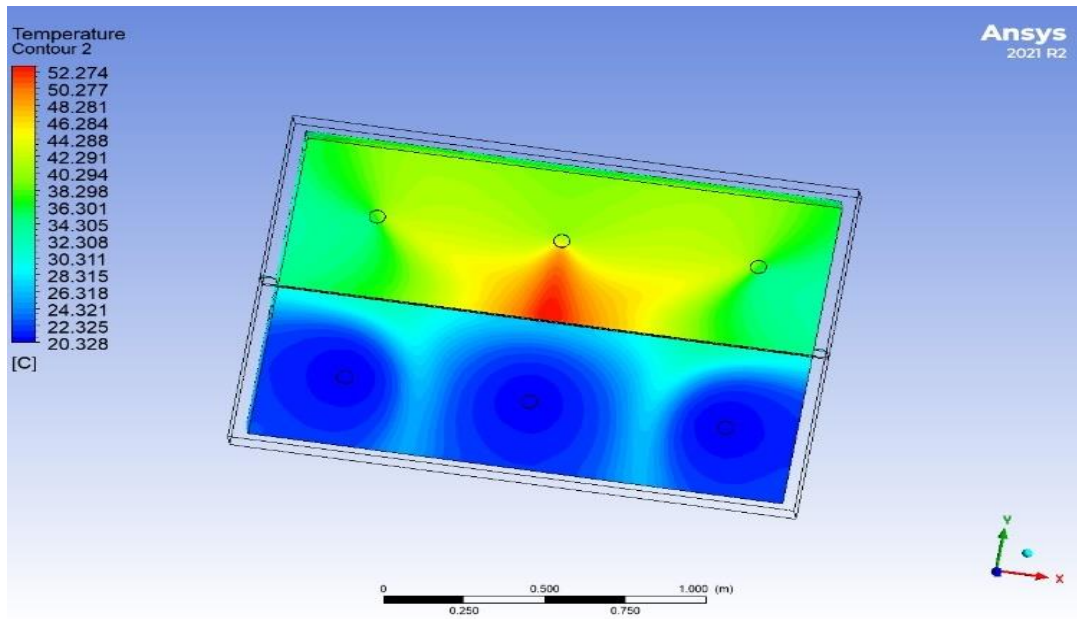


Figure 3.22. Temperature distribution for generator in 20°C in 0.001m/s.

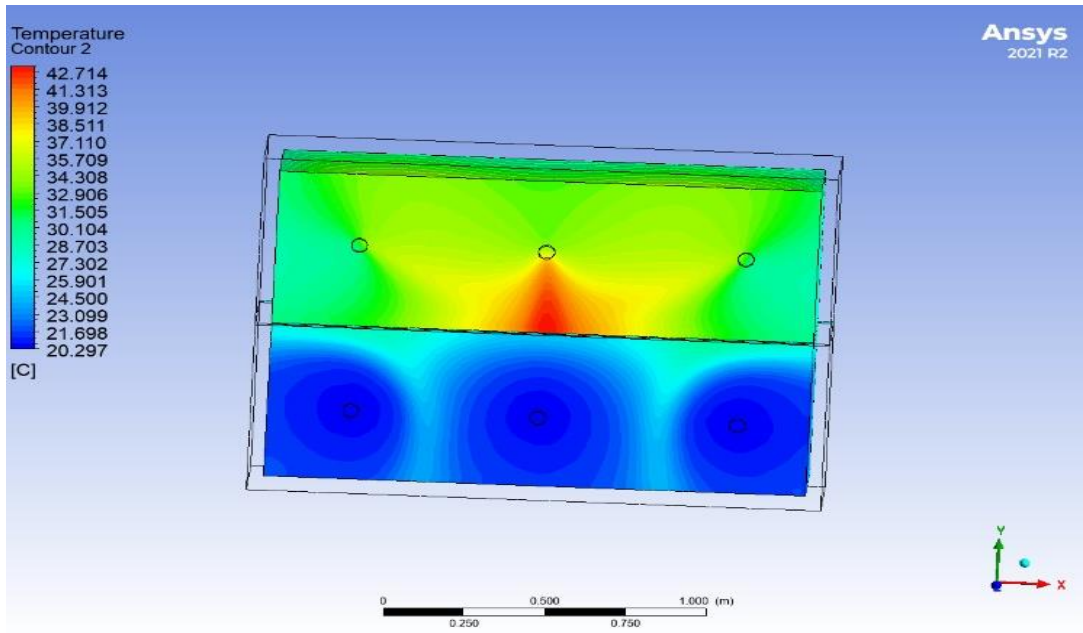


Figure 3.23. Temperature distribution for generator in 20°C in 0.0015m/s.

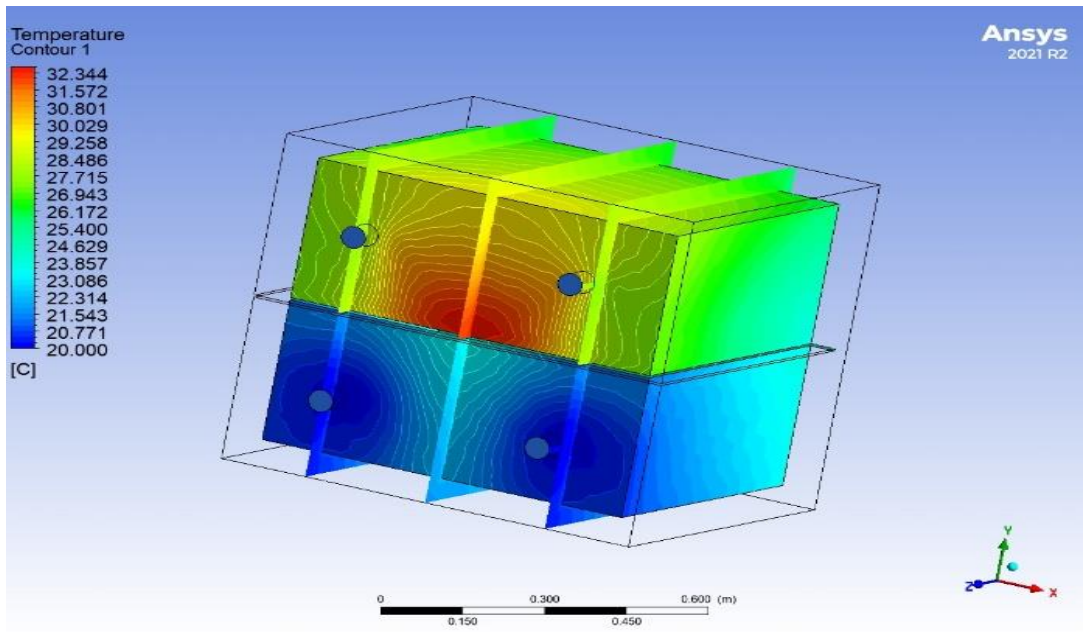


Figure 3.24. Temperature distribution for gearbox in 20°C in 0.0005m/s.

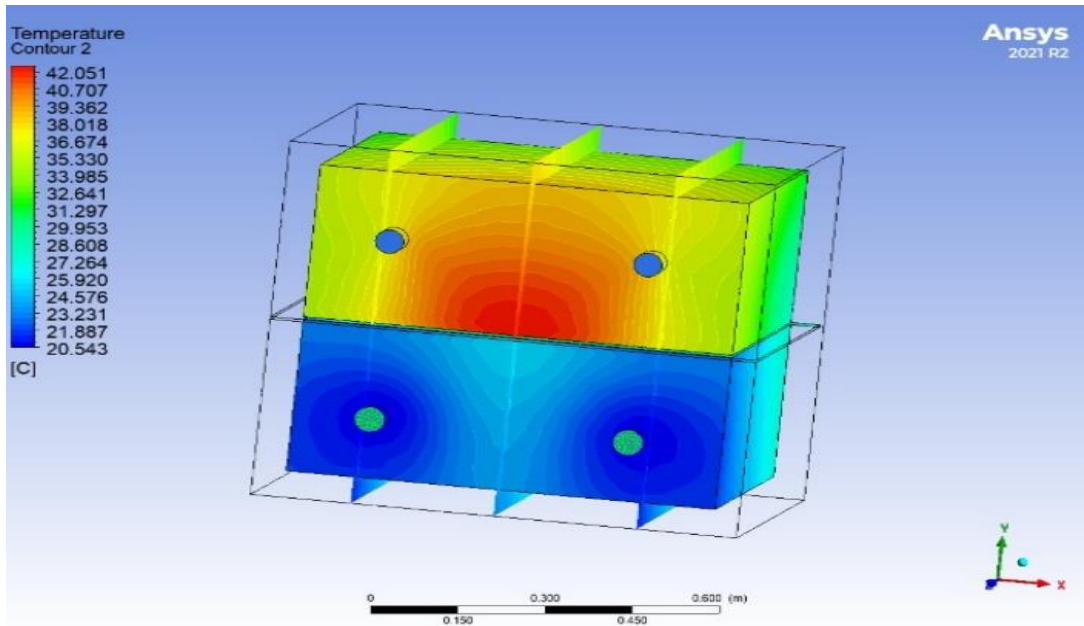


Figure 3.25. Temperature distribution for gearbox in 20°C in 0.001m/s.

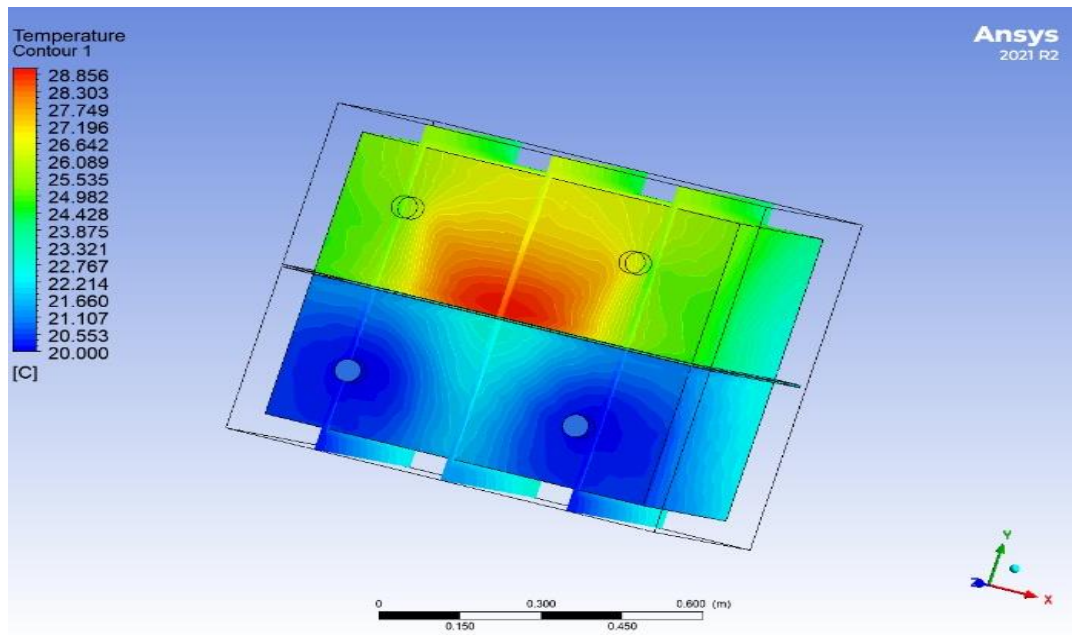


Figure 3.26. Temperature distribution for gearbox in 20°C in 0.0015m/s.

3.3.2. Liquid Temperature 30 °C

The generator and gearbox received the same heat flow in this simulation, but the amount of water and oil entry temperature was changed, as well as the usage of three different velocities, to achieve good cooling under these conditions. After performing the simulation of three different velocity for water and oil. the following temperature results were obtained:

Table 3.8. Temperature data for liquid cooling 30 °C.

Velocity m/s	Gearbox (°C)	Generator(°C)
0.0005	40	51
0.001	35	41
0.0015	35	37

It is noticeable from the readings that liquid cooling works well in the study's conditions. Liquid cooling has been found to be more effective than forced air cooling, although the nacelle's insulation must be good because excessive heat can reduce cooling effectiveness. Additionally, we observe a slow rise in velocity that brings the gearbox and generator's temperature down. To further prove this, the mass flow rate and heat transfer rate were theoretically calculated. Figure 16&17 shows that increasing mass flow rate of water and oil flowing decreases the temperature. Figure 18 & 19 also shows that the amount of heat transferred abroad gradually decreases as the amount of flow increases. Since there is no time for the heat to escape to the outer atmosphere, temperatures within the vehicle remain constant.

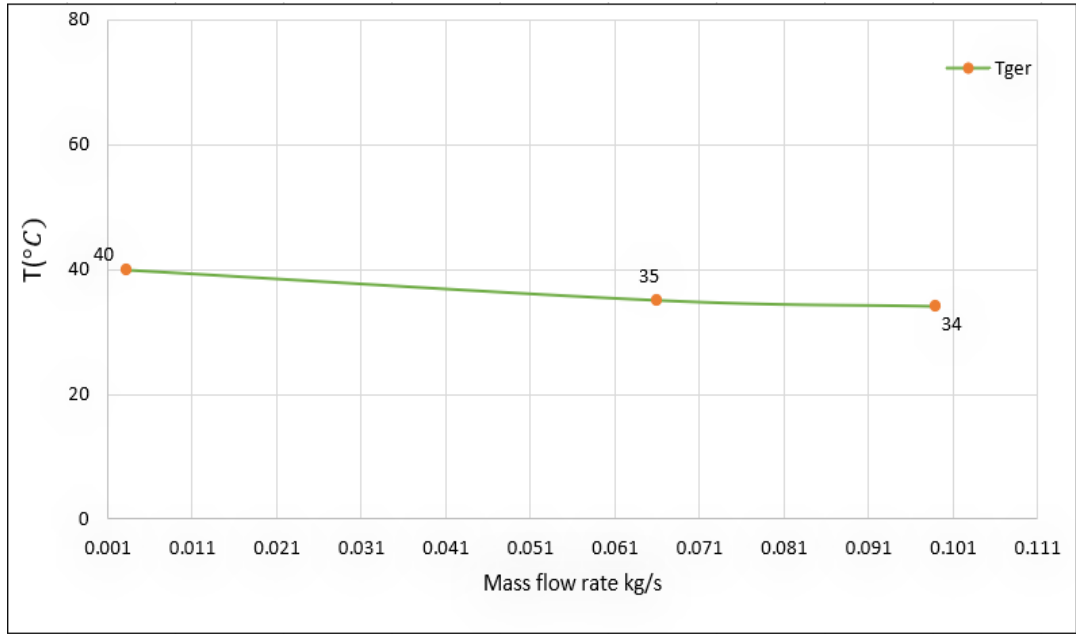


Figure 3.27. Variation of mass flow (Kg/s) rate and temperature for gearbox (°C).

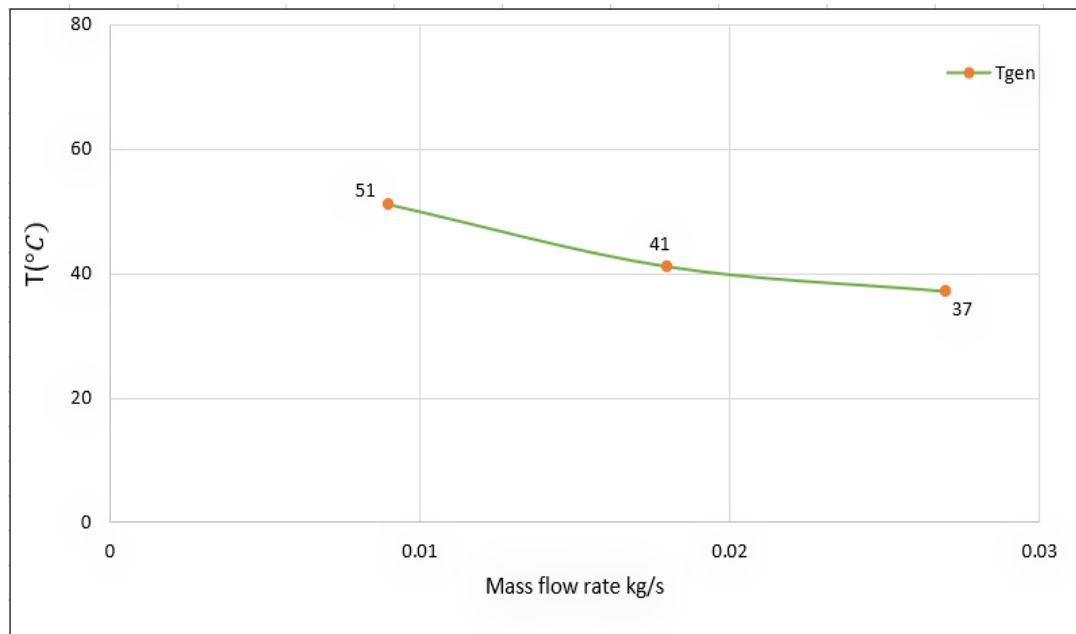


Figure 3.28. Variation of mass flow rate (Kg/s) and temperature for generator (°C).

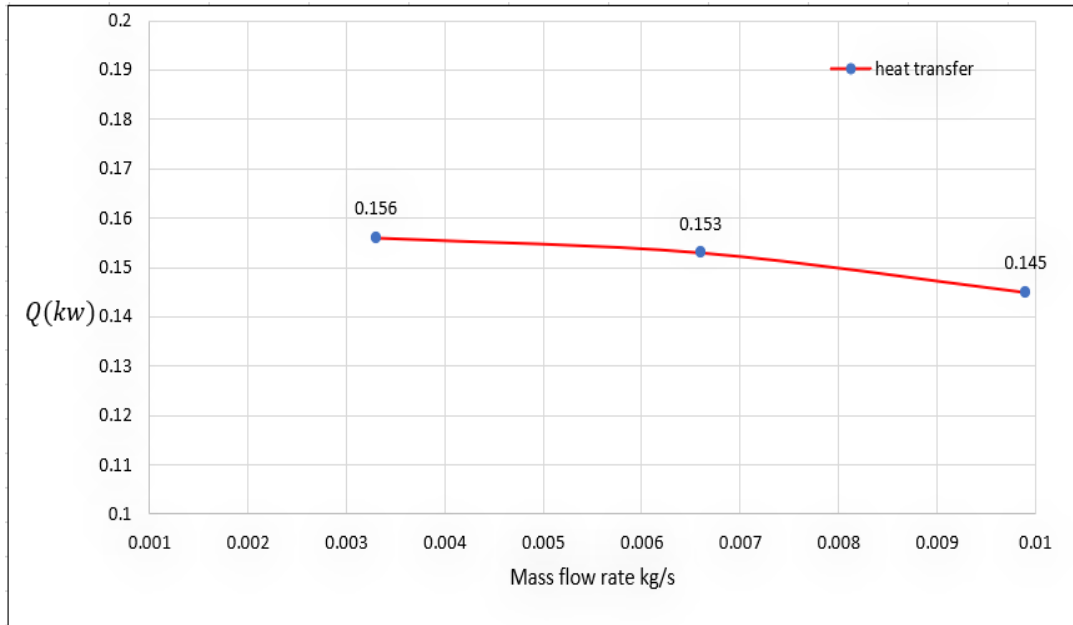


Figure 3.29. Variation of mass flow rate (Kg/s) for oil and heat transfer (kw).

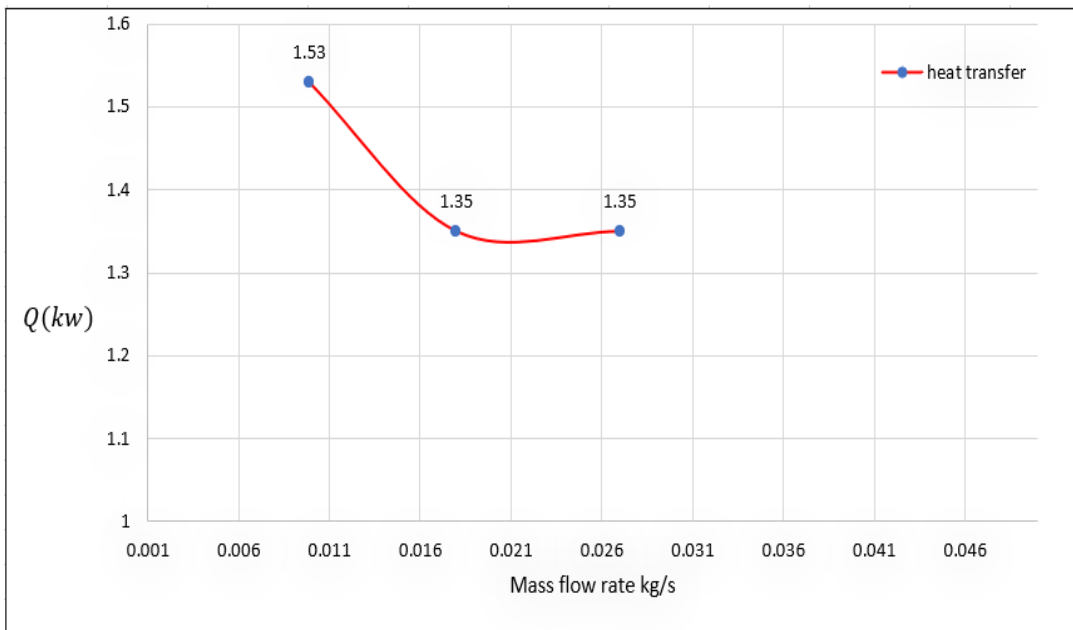


Figure 3.30. Variation of mass flow rate (Kg/s) for water and heat transfer (kw).

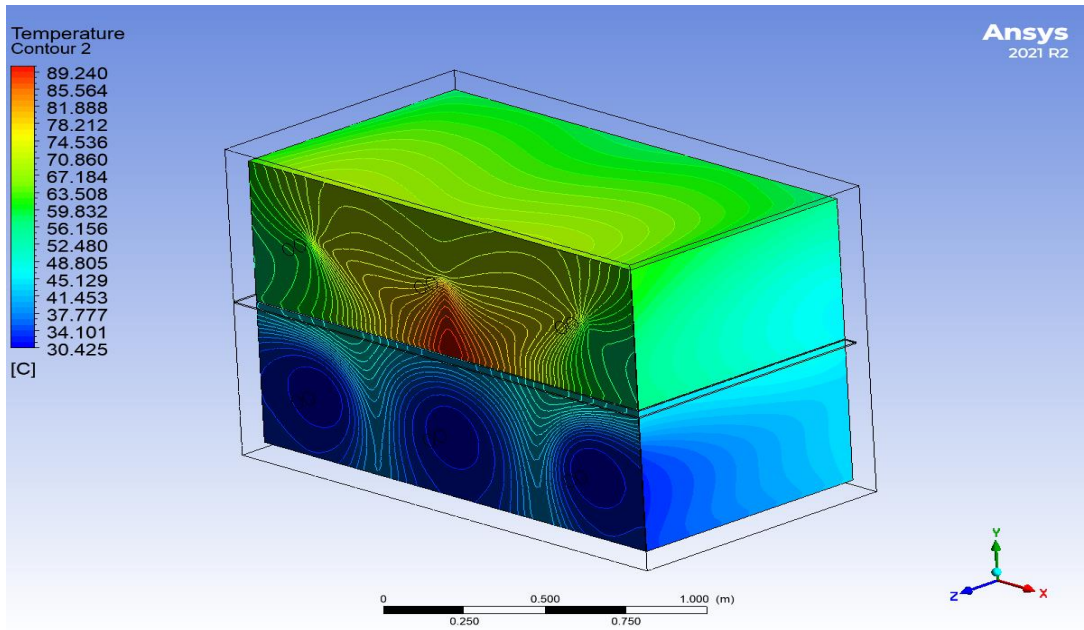


Figure 3.31. Temperature distribution for generator 30°C in 0.0005 m/s.

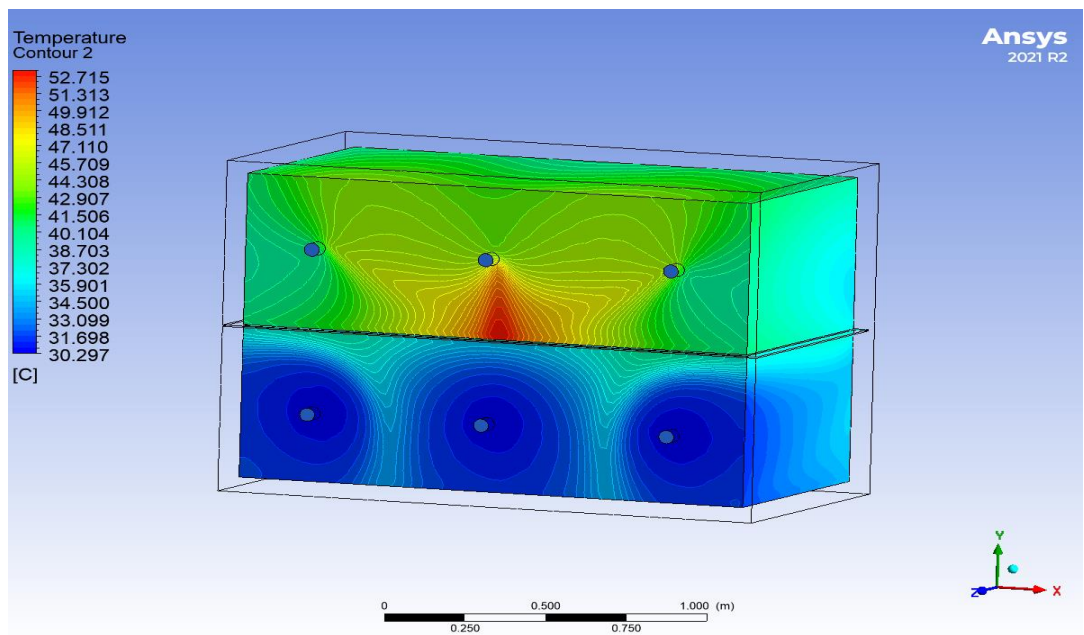


Figure 3.32. Temperature distribution for generator 30°C in 0.001m/s.

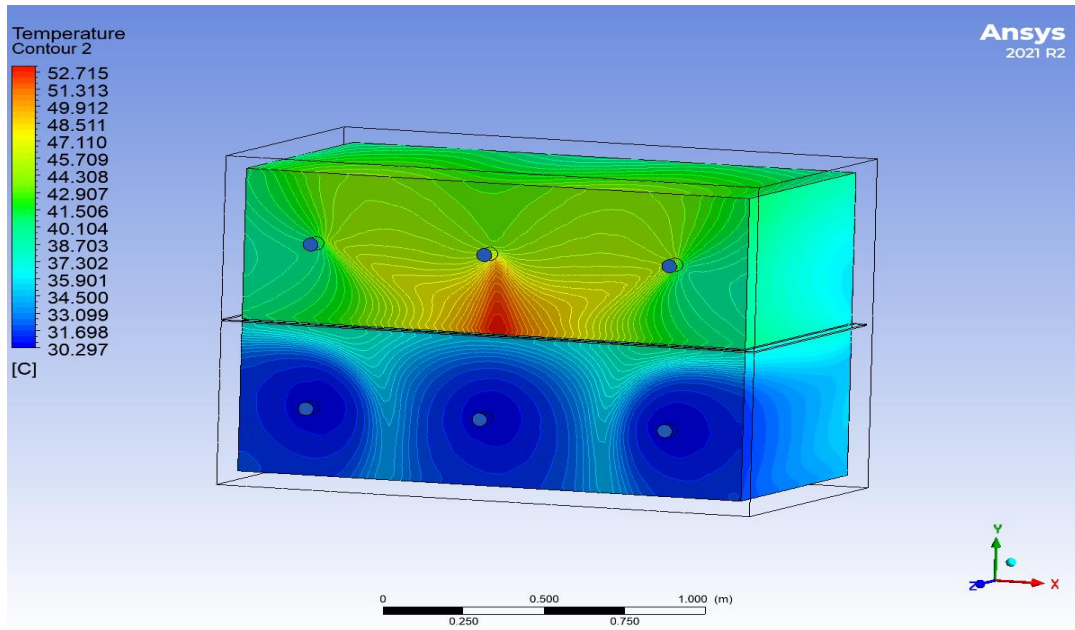


Figure 3.33. Temperature distribution for generator 30°C in 0.0015m/s.

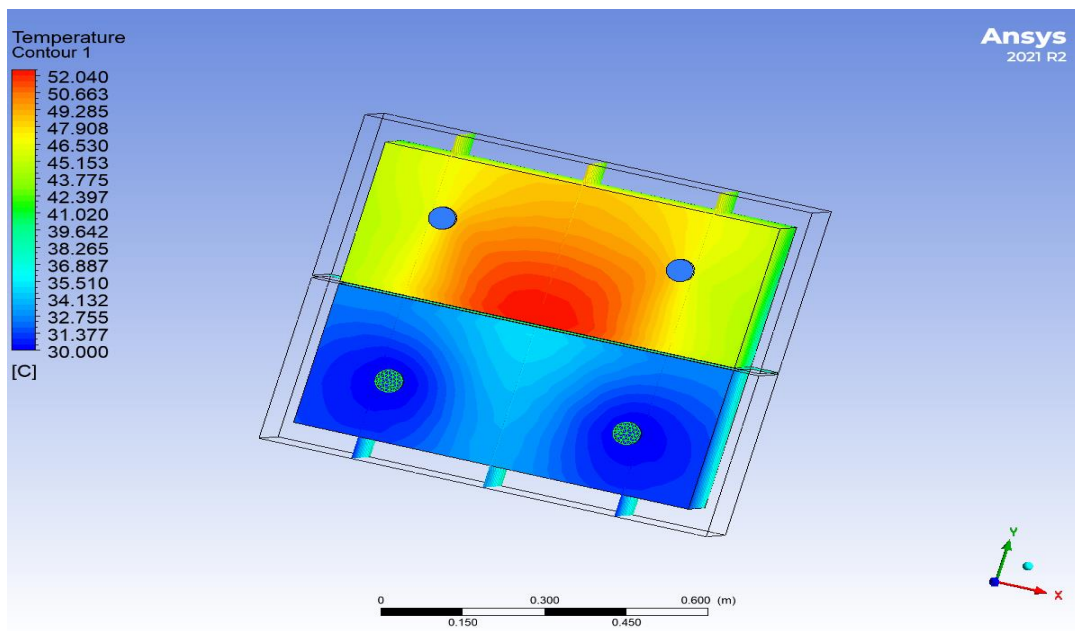


Figure 3.34. Temperature distribution for gearbox 30°C in 0.0005m/s.

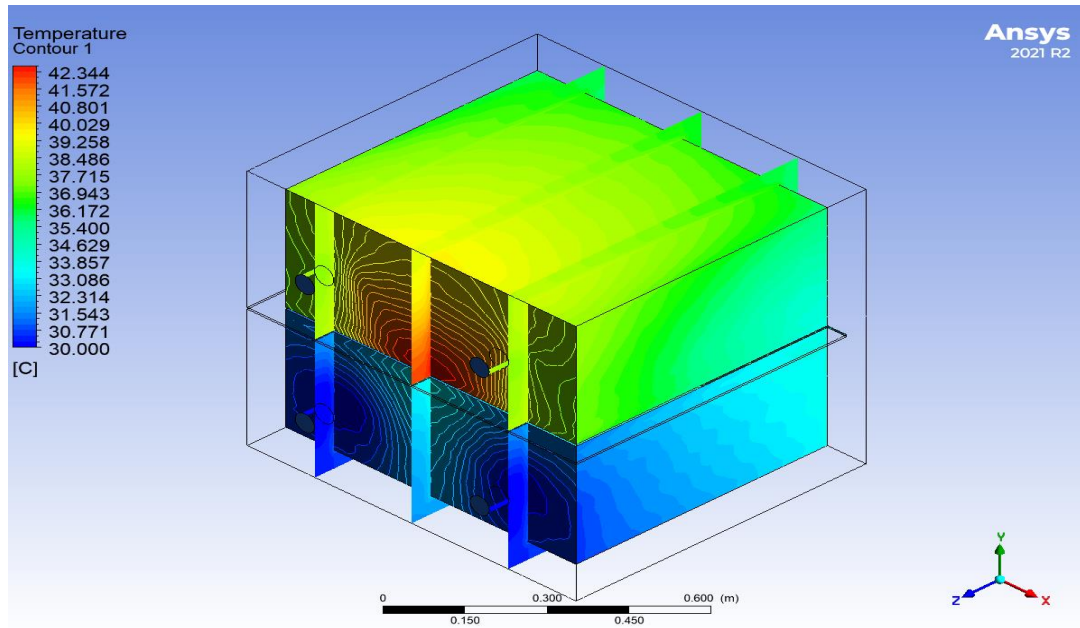


Figure 3.35. Temperature distribution for gearbox 30°C in 0.001m/s.

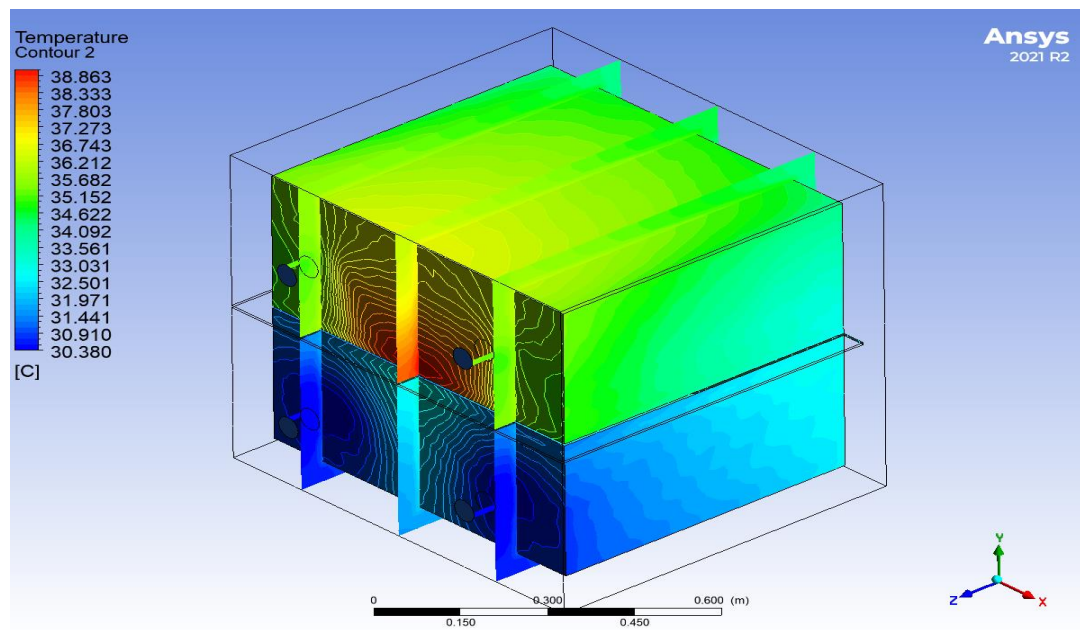


Figure 3.36. Temperature distribution for gearbox 30°C in 0.0015.

3.3. COMPARISON BETWEEN THE RESULTS FOR AIR FORCED COOLING SYSTEM AND LIQUID COOLING SYTEM

The simulation findings indicated that liquid cooling is preferable to forced air cooling. Liquid cooling is more expensive, thus wind turbines in cold or medium temperatures don't need to employ it. The electrical and mechanical components housed within the nacelle can be kept cool with just the use of forced air conditioning. Mechanical and electrical equipment requires additional cooling while operating in hot environments. So, it's evident that forced air cooling isn't effective and isn't enough to keep the nacelle equipment cool. The results of liquid cooling and forced air cooling were graphed for clarity. The graph below shows the difference in temperature between the generator after being cooled with forced air versus liquid.

Figure 3.25 depicts our discovery that liquid cooling the generator using a jet cooler improves from forced air cooling around 20%. In this case, the generator was cooled by forced and liquid air at an input temperature of 20°C.

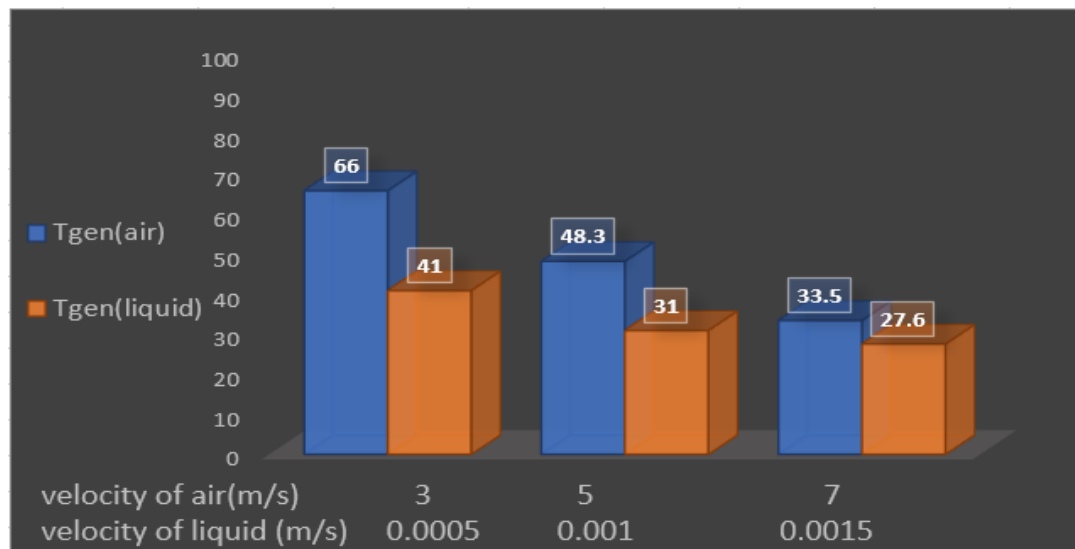


Figure 3.37. Comparison between the temperature of the generator cooled by the air forced system and the liquid cooling system.

Figure 3.26 demonstrates that when the inlet temperature of the liquid is 30°C, the results are acceptable and reliable in cooling the generator, which produces 1 (MW) of power. This is in contrast to the case when cooling with forced air at a temperature of 40°C excretes us with a very high temperature of the generator. It was pointed out that the variation can reach 20%.

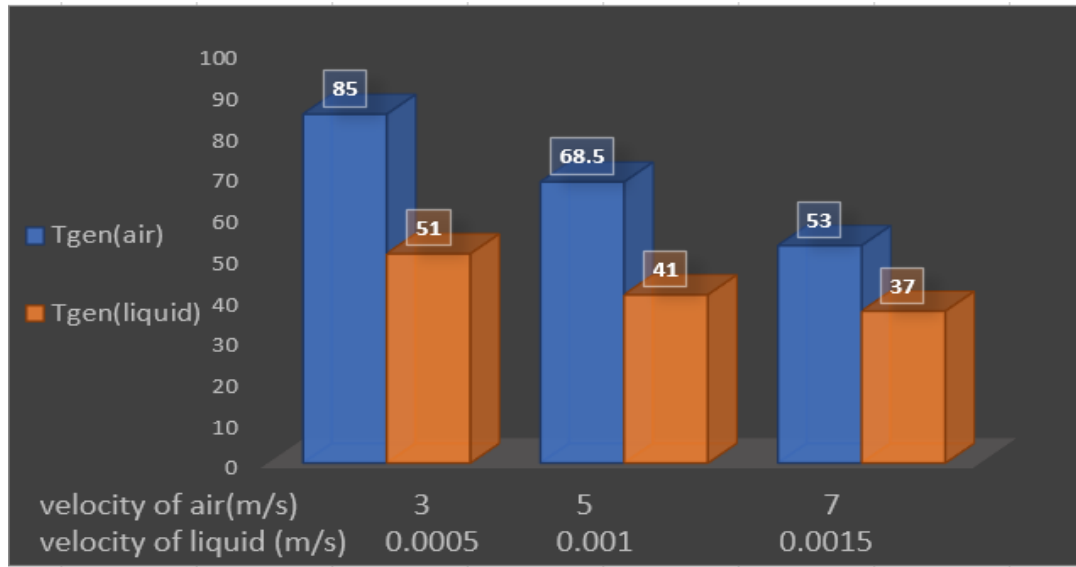


Figure 3.38. Comparison between the temperature of the generator cooled by the air forced system and the liquid cooling system.

Liquid cooling was found to create a more tolerable temperature for the gearbox than forced air cooling. Using an assumed inlet air and liquid temperature of 20°C, the findings were laid out for us in Figure 3.27.

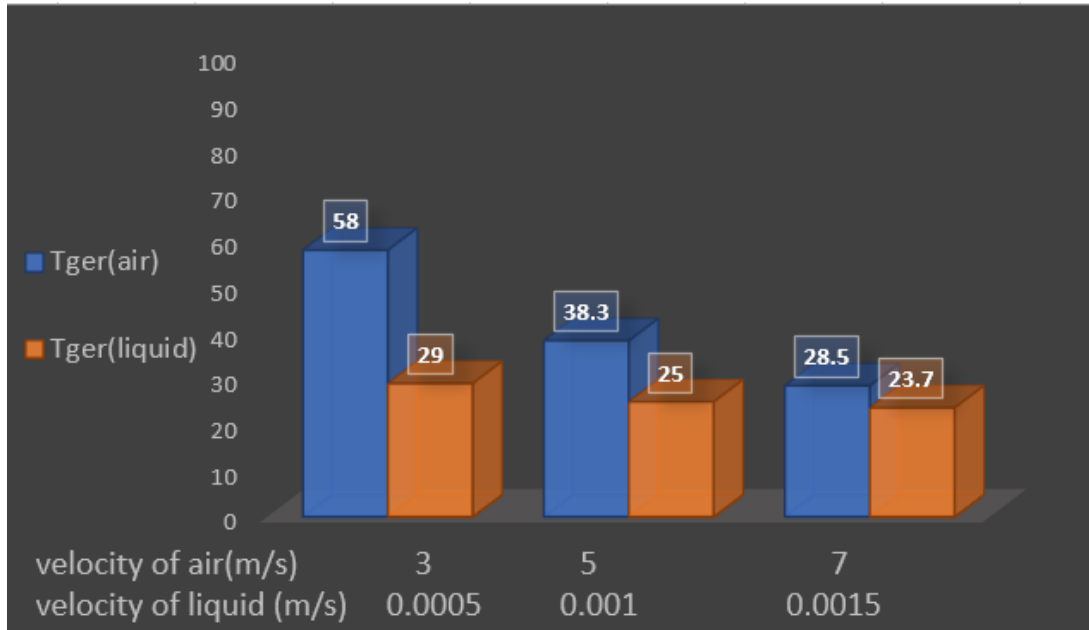


Figure 3.39. Comparison between the temperature of the gearbox cooled by the air forced system and the liquid cooling system.

In the second scenario, a considerable temperature increase was observed when cooling with forced air but was tolerable when cooling with liquid, with the air inlet temperature set at 40 °C and the liquid inlet temperature set at 30°C. This is depicted in Figure (3.28).

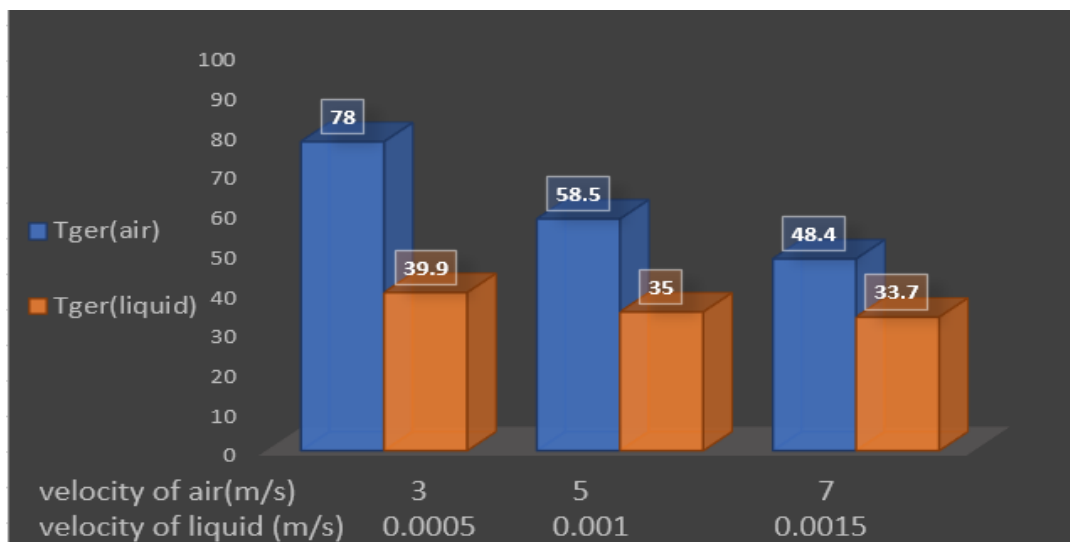


Figure 3.40. Comparison between the temperature of the gearbox cooled by the air forced system and the liquid cooling system.

PART 4

CONCLUSION

This research compared the efficiency of cooling mechanical and electrical components inside the nacelle with forced air-cooling system and liquid cooling system. this study's objective is to identify the most effective strategy for cooling the Nacelle generator and gearbox. cooling mechanical and electrical devices by the use of CFD simulations performed in ANSYS-Fluent (2021- R1). Wind turbines should be constructed so that they can operate in very high winds. It's a matter of the climate A conflicting design need arises from the fact that electrical and mechanical components may be exposed to extremely high temperatures within the nacelle temperature gradients. With the use of CFD software, we have solved the Navier-Stokes equations (NSE) for fluid flow, which account for the fluid's continuity, momentum, and energy. As part of the thermal equilibrium equation for a wind turbine, we need a thermodynamic description of the entire system's heat. Therefore, based on the results of the simulations, liquid cooling is superior to forced air cooling. Wind turbines operating in cold or moderate climates don't need to use liquid cooling because of the higher cost associated with doing so. The nacelle's mechanical and electrical components can be cooled using merely air conditioning. Working in hot conditions necessitates the use of supplemental cooling for mechanical and electrical equipment. As a result, it is clear that the nacelle equipment cannot be kept cold by forced air cooling alone. It was also found that the generator and gearbox cooled down better when subjected to a higher volume of forced or liquid air. The studies also showed that going faster results in less heat being transported. The results and simulations showed that liquid cooling is superior to forced air cooling.

4.1. SUGGESTIONS FOR FUTURE STUDY

In the future, researchers will likely concentrate on creating a more precise numerical method that accounts for the vast majority of relevant practical and nacelle thermal design factors, such as the impact of radiation heat exchange, the modeling of heat generation (due to generator, gearbox, and electronic components), and the three-dimensional flow fields inside the nacelle and around the wind turbine. There are many suggestions that we will describe some of them for a more efficient and less expensive cooling system:

- The most cost-effective cooling method is forced air, which requires only the installation of a heat exchanger to cool the air before it enters the nacelle in hot locations.
- High-yield wind turbines can benefit from the use of more than one fan for efficient cooling in mild climates, while hotter regions will require the addition of a heat exchanger to pre-cool the air before it enters the nacelle.
- A larger heat exchanger is required to effectively cool the generator and gearbox with a single liquid.
- Nanofluid can be used to cool mechanical and electrical components in wind turbines producing more than 5MW.

REFERENCE

1. Kehinde, O., Babaremu, K. O., Akpanyung, K. V., Remilekun, E., Oyedele, S. T., and Oluwafemi, J., "Renewable energy in Nigeria - A review", **International Journal Of Mechanical Engineering And Technology**, 9 (10): 1085–1094 (2018).
2. Mechanics, F., "THERMAL ANALYSIS OF WIND TURBINE NACELLE OF 2 . 5 MW TURBINES AT WINTER CONDITIONS Kadir Nuri Tekin , Tahir Yavuz and Emre Koç", (July): 1971–1977 (2014).
3. De Risi, A., Milanese, M., Colangelo, G., and Laforgia, D., "High efficiency nanofluid cooling system for wind turbines", **Thermal Science**, 18 (2): 543–554 (2014).
4. Christensen, V., "Ecopath with Ecosim: linking fisheries and ecology 1 Why ecosystem modeling in fisheries?", **WIT Transactions On State Of The Art In Science And Engineering**, 34: 1755–8336 (2009).
5. Smaili, A., Mahdi, M. A., and Ouahchia, L. M., "Numerical Investigations of Free-Convection within Wind Turbine Nacelle Operating in Hot Climate", 148–152 .
6. Bhamare, N. and Gadhe, P. P., "Thermal Analysis of Wind Turbine Nacelle using OpenFoam", 10 (7): 393–397 (2019).
7. FUSKELE, V., Baredar, P., Sarviya, R. M., Lal, S., Gupta, B. L., and Awasthi, S., "Numerical Investigation of Wind Turbine Nacelle Cooling with Al₂O₃ Nanofluid", **SSRN Electronic Journal**, 1–7 (2021).
8. Mahdi, M. A. and Smaili, A., "Numerical investigations of laminar buoyant heat transfer in a 2D-enclosure - Application to wind turbine nacelle operating in hot climate", **Mechanika**, 23 (5): 667–672 (2017).
9. Smaili, A., Masson, C., Taleb, S. R., and Lamarche, L., "Numerical study of thermal behavior of a wind turbine nacelle operating in a nordic climate", **Numerical Heat Transfer, Part B: Fundamentals**, 50 (2): 121–141 (2006).
10. Patel, A. and Dhakar, P. S., "CFD Analysis of Air Conditioning in Room Using Ansys Fluent", **Journal Of Emerging Technologies And Innovative Research**, 5 (11): 436–441 (2018).
11. Pechanek, R. and Bouzek, L., "Analyzing of two types water cooling electric motors using computational fluid dynamics", **15th International Power Electronics And Motion Control Conference And Exposition, EPE-PEMC 2012 ECCE Europe**, 2–6 (2012).

12. Tskhvirashvili D.G., Berishvili Z.D., Keshelava V.G., Tsagareli K., Experience in operating the water-cooling system of the generator stator windings at the inguri hydroelectric station, *Power Technology and Engineering (Formerly Hydro Technical Construction)*, 24(8): 23-24, (1990).
13. Sheng, J., Meng, X., Chu, S., and Guo, H., "Review of the Cooling Technology for High-power Wind Turbines", (*Icadme*): 1798–1803 (2015).
14. Xydis, G., Pechlivanoglou, G., and Nayeri, N., "Wind Turbine Waste Heat Recovery—A Short-Term Heat Loss Forecasting Approach", **Challenges**, 6 (2): 188–201 (2015).
15. Tripathy, S., "A Case Study of Different Generator Topologies used in Wind Turbine Applications DIFFERENT GENERATOR TURBINE APPLICATIONS", (August): 0–27 (2016).
16. Smaili, A. and Mahdi, M. A., "On Clean Cooling Systems for Wind Turbine Nacelle operating in Hot Climate On Clean Cooling Systems for Wind Turbine Nacelle operating in Hot Climate", (April 2016): 0–7 (2015).
17. Barakos, G., Mitsoulis, E., and Assimacopoulos, D., "Natural convection flow in a square cavity revisited: Laminar and turbulent models with wall functions", **International Journal For Numerical Methods In Fluids**, 18 (7): 695–719 (1994).
18. Smaili, A., Tahri, A., and Masson, C., "Thermal analysis of wind turbine nacelle operating in Algerian Saharan climate", **Energy Procedia**, 18: 187–196 (2012).
19. Furuse, M., Fuchino, S., Okano, M., Natori, N., and Yamasaki, H., "Development of a cooling system for superconducting wind turbine generator", **Cryogenics**, 80: 199–203 (2016).
20. Mahdi, M. A., Smaili, A., and Lakehal, D., "Thermal Analysis of HAWT-Nacelle operating in Hot Climate Regions using CFD code TransAT", 2: 15–17 (2013).
21. Laakso T., Holttinen H., Ronsten G., Tallhaug L, Horbaty R., Baring-Gould I., Lacroix A., Peltola E. And Tammelin B. "State-of-the-art of wind energy in cold climates", IEA, April 2003.
22. A. N. Ibrahim, "Developing Turbulent Flow and Heat Transfer Through Rectangular and Circular Duct Cross Section," M.sc. thesis Mechanical Engineering Department, University of Babylon, 2005.
23. H. K. Versteeg and W. Malalasekera, *An introduction to computational fluid dynamics: the finite volume method*: Pearson Education, 2007.
24. Tran L. D., Masson C. and Smaili A., A Stable Second-Order Mass-Weighted Upwind Scheme for Unstructured Meshes, *International Journal for Numerical Methods in Fluids*, (2006), Vol. 51, pp 749-771.

25. Wang Li, Haifeng Wang, Steady-state thermal simulation of the stator coil of the evaporative inner cooling system in wind turbines, *Information and Automation for Sustainability*, 2012: 248-251.
26. G.Barakos, E.Mitsoulis and D.Assimacopoulos "Natural Convection Flow in a Square Cavity Revisited: Laminar and Turbulent Models with Wall Functions", *International Journal for numerical methods in fluids*, vol.18, pp (695-719), 1994.
27. B. E. Launder and D. B. Spalding, "The numerical computation of turbulent flows," in *Numerical prediction of flow, heat transfer, turbulence and combustion*, ed: Elsevier, 1983, pp. 96-116.

RESUME

My name Abdulkhaleq Salman MWEA, I have graduated from wasit University/College of mechanical engineering 2014-2018. After graduating I worked two years in power plant station. Then in 2020, I started master degree at Karabuk University.